quaternary

MDPI

Article

Unveiling the Volcanic History of Ancient Pompeii (Italy): New Insights from the Late Pleistocene to Holocene (Pre-79 CE) Stratigraphy

Domenico Sparice [1,2,*], Mauro Antonio Di Vito [1], Vincenzo Amato [2,3], Valeria Amoretti [4], Alessandro Russo [4], Pierfrancesco Talamo [5] and Gabriel Zuchtriegel [4]

1 Istituto Nazionale di Geofisica e Vulcanologia, Sezione di Napoli "Osservatorio Vesuviano", Via Diocleziano 328, 80124 Naples, Italy; mauro.divito@ingv.it
2 Laboratorio di Ricerche Applicate "A. Ciarallo", Parco Archeologico di Pompei, Via Plinio 26, 80045 Pompei, Italy; vincenzo.amato@unimol.it
3 Dipartimento di Bioscienze e Territorio, Università del Molise, Contrada Fonte Lappone, 86090 Pesche, Italy
4 Ministero della Cultura, Parco Archeologico di Pompei, Via Plinio 26, 80045 Pompei, Italy; valeria.amoretti@cultura.gov.it (V.A.); alessandro.russo@cultura.gov.it (A.R.); gabriel.zuchtriegel@cultura.gov.it (G.Z.)
5 Ministero della Cultura, Parco Archeologico dei Campi Flegrei, Rione Terra, 80078 Pozzuoli, Italy; pierfrancesco.talamo@cultura.gov.it
* Correspondence: domenico.sparice@ingv.it

Abstract: Many volcanological and geoarchaeological studies in the ancient city of Pompeii (Italy) have been devoted to the 79 CE Plinian eruption of Vesuvius, which sealed the city under a thick pyroclastic sequence. Only fragmentary information exists regarding the stratigraphy of the volcanic sediments sandwiched between the 79 CE street level and the volcanic rocks that form the geological framework of the hill on which Pompeii was built, which constitutes the "Pompeii bedrock". The stratigraphic survey of twenty-one trenches throughout the city, coupled with a geochemical characterization, highlighted that the pre-79 CE stratigraphy includes at least eight late Pleistocene to Holocene tephra layers. Six eruptions were sourced from Somma–Vesuvius (Pomici di Base, Mercato, AP1 to AP4) and two originated from Campi Flegrei (Neapolitan Yellow Tuff and Soccavo 4). The Pompeii bedrock is the product of local vents, the last activity of which possibly shortly predates the 22 ka Pomici di Base eruption. From a geoarchaeological perspective, a relevant result is the absence of the 3.9 ka Avellino tephra in all trenches. This evidence, along with the reappraisal of the stratigraphy of the nearby archaeological site of S. Abbondio, suggests that the Avellino eruption possibly only marginally affected the Pompeii area during the Early Bronze Age.

Keywords: Pompeii archaeological site; 79 CE eruption; S. Abbondio site; chronostratigraphy; geoarchaeology; Bronze Age; Avellino eruption; AP eruptions; Somma–Vesuvius; Campi Flegrei

check for updates

Academic Editor: C. Neil Roberts

Received: 22 October 2024
Revised: 23 December 2024
Accepted: 15 January 2025
Published: 21 January 2025

Citation: Sparice, D.; Di Vito, M.A.; Amato, V.; Amoretti, V.; Russo, A.; Talamo, P.; Zuchtriegel, G. Unveiling the Volcanic History of Ancient Pompeii (Italy): New Insights from the Late Pleistocene to Holocene (Pre-79 CE) Stratigraphy. *Quaternary* **2025**, *8*, 4. https://doi.org/10.3390/quat8010004

Copyright: © 2025 by the authors. Licensee MDPI, Basel, Switzerland. This article is an open access article distributed under the terms and conditions of the Creative Commons Attribution (CC BY) license (https://creativecommons.org/licenses/by/4.0/).

1. Introduction

Many times, throughout history, from the distant past to modern times, volcanic eruptions have disrupted human settlements and activities (e.g., [1–4]). The combination of geological and archaeological investigations provides essential information on the effects of eruptions on humans and how communities recovered and, possibly, resettled in the same area after volcanic events (e.g., [5–8]). This is especially true for the Neapolitan volcanic area (Campania, southern Italy), which includes three active volcanoes: Somma–Vesuvius, Campi Flegrei and Ischia Island (Figure 1). The history of these peri-contemporaneous

volcanoes is intertwined with that of the communities that have been living in these areas for millennia [4,9–12], with both beneficial and detrimental implications [2,3]. Villages have thrived due to the fertility of the volcanic soils and the availability of natural resources and, on the other hand, suffered the catastrophic consequences of the eruptions. One of the most famed examples is the ancient city of Pompeii, located 9.5 km southeast of the current Vesuvius crater, in the central–northern sector of the Sarno alluvial–coastal plain (Figure 1). Ancient Pompeii is inextricably linked to the 79 CE Plinian eruption of Vesuvius, not surprisingly known as the "Pompeii" eruption, which ravaged the city and preserved its ruins under a blanket of pyroclastic deposits. The city was struck by a Plinian fallout followed by a series of pyroclastic currents, which resulted in widespread devastation and deaths [13–22]. Pompeii has become one of the world's most famous archaeological sites and an unparalleled source of information on many aspects and consequences of the 79 CE eruption, such as the effects of the syn-eruptive seismicity on buildings and inhabitants [23] or the genetic and family relationships and sexes of groups of victims [24], which partially refute traditional interpretations of gendered behaviors in facing the catastrophe. Nonetheless, the close association of volcanic activity and a human presence in the Pompeii area has its roots in the Early Bronze Age (EBA) and late Neolithic, long before the founding of the city, whose first urban nucleus dates to the archaic period, between VIII and VI centuries BCE [25] (p. 13) [26] (p. 82). The human presence in the Pompeii area is evidenced by the finding, in trenches dug for archaeological investigation, of pottery fragments belonging to EBA Palma Campania culture [27,28], in association with a tephra layer speculatively attributed to the 3.9 ka Avellino Plinian eruption (Somma–Vesuvius), and material fragments of the late Neolithic Diana culture [29], distributed through southern Italy between 4300 and 3700 BCE [30], incorporated into the paleosol developed on the pyroclastic deposits of the 8.9 ka Mercato Plinian eruption (Somma–Vesuvius).

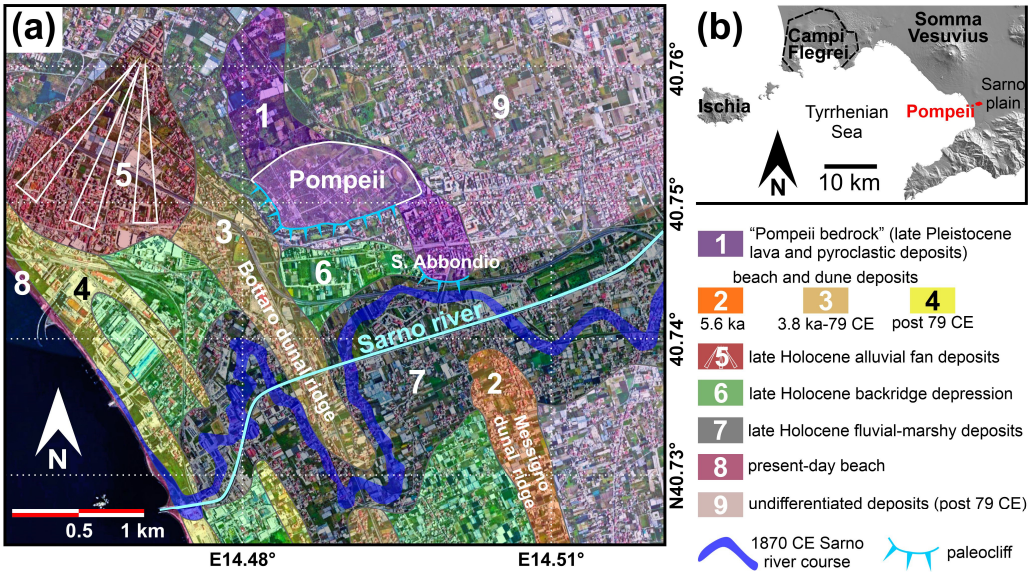

Figure 1. (**a**) Geological map of the Sarno plain to the south of Pompeii (data from [31,32]). (**b**) Location of Pompeii in the Sarno plain, to the southeast of the Somma–Vesuvius volcano; the other Neapolitan volcanoes (Campi Flegrei caldera and Ischia Island) are shown as well.

While the paleoenvironmental and landscape evolution of the plain surrounding ancient Pompeii, even in response to volcanic activity, has been thoroughly investigated (e.g., [32–44]), few geoarchaeological studies [45–50] have been devoted to the late Pleistocene to Holocene (pre-79 CE) stratigraphy within the city walls, with scarce information about the structural/textural/sedimentological characteristics of the volcanic deposits and

intervening materials. Only recently, Amato [51] provided a geoarchaeological stratigraphy that includes general descriptions of several pre-79 CE tephra layers recognized in trenches dug in the central part of Pompeii.

Unfortunately, the attribution of pre-79 CE tephra layers to specific eruptions has often been made without any robust volcanological constraints. In addition, reworking and extensive anthropic activity (cuts and infills) have further complicated the interpretation of the volcanic stratigraphic record. This study provides insights into the pre-79 CE volcanic chronostratigraphy of Pompeii by means of a detailed stratigraphic survey, coupled with a geochemical characterization, of tephra layers recognized in twenty-one trenches dug below the 79 CE street level in different parts of the city. The main case study is represented by twelve trenches (CA1 to CA12) in the so-called Insula dei Casti Amanti (Figure 2). Four other trenches (S1 to S4) were investigated in insula 16 of Regio I (Figure 2), while the remaining five trenches are located as follows (Figure 2): Villa dei Misteri (VM), insula 2 of Regio VIII (S30), Foro Triangolare (FT), Tempio di Iside (IsT) and the eastern end of via dell'Abbondanza (S16). We aimed to reconstruct the late Pleistocene to Holocene chronostratigraphic evolution of the Pompeii site through a chronologically well-constrained sequence of volcanic eruptions, separated by phases of quiescence during which pedogenesis and reworking/erosional processes resulted in the formation of well-developed paleosols, reworked volcaniclastic materials and/or sub-aerial erosional surfaces. Our chronostratigraphic reconstruction may also be useful for future archaeological investigations of pre-Roman layers in Pompeii, as tephra layers represent the result of geologically instantaneous events (volcanic eruption) and, consequently, are isochronous surfaces that can be used for a relative dating of archaeological finds, occupation levels or archaeologically barren materials.

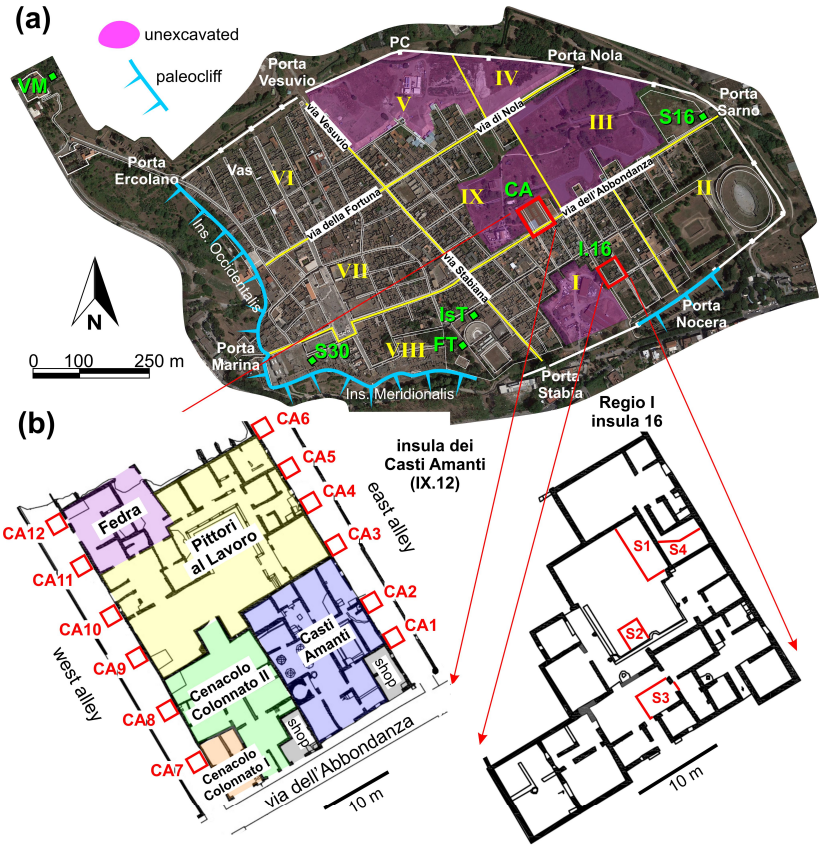

Figure 2. (**a**) Map of Pompeii with subdivision in *regiones*, indicated by Roman numerals (I–IX), and *insulae* (white blocks). The paleocliff contour is from Amato et al. [41]. Locations of trenches: CA

(Insula dei Casti Amanti; trenches CA1 to CA12), I.16 (Regio I, insula 16; trenches S1 to S4), VM (Villa dei Misteri), S30 (Regio VIII, insula 2), FT (Foro Triangolare), IsT (Tempio di Iside) and S16 (eastern end of via dell'Abbondanza). Locations described in the text are also reported: Vas = Casa dei Vasi di Vetro; PC = area of the so-called Porta Capua. (**b**) Plan view of the Insula dei Casti Amanti and the southern sector of I.16 (modified after D'Auria [52]), with the positions of the investigated trenches. The housing units that compose the Insula dei Casti Amanti are highlighted with different colors.

2. Pompeii Archaeological Site and the Insula dei Casti Amanti

The ancient city of Pompeii extends over an area of about 66 hectares (Figure 2). About two-thirds of the city have been unearthed following the early excavations started in 1748. The city is surrounded by massive walls punctuated by twelve defense towers and seven gates (Porte in Italian) (Figure 2). The current urban planning of Pompeii, conceived in the mid-19th century by the archaeologist Giuseppe Fiorelli [25] (p. 33) [53] (p. 34), is divided in nine large districts, called "regiones" (singular Regio) and indicated by Roman numerals (I–IX), bounded by thoroughfares. Each Regio is further subdivided in many blocks, called "insulae", bounded by alleys. The Insula dei Casti Amanti is numbered insula 12 in Regio IX and faces south onto via dell'Abbondanza (Figure 2). An early excavation of the insula was initiated in the early 1910s by the archaeologist Vittorio Spinazzola [54], during which the façades of buildings fronting the via dell'Abbondanza were brought to light. A systematic excavation campaign started in 1987, continued in various phases [55,56], and is still ongoing. As a result, the southern part of the insula has been unearthed as well as the alleys that flank it. The current campaign includes the re-profiling and stabilization of the excavation fronts and the building of a new covering, a single-span steel truss with suspended walkways, replacing the old roofing system [57–59].

3. The Neapolitan Volcanic Area

Located to the east of the Neapolitan volcanoes (Figure 1), Pompeii lies within the easterly dispersal of the pyroclastic products pertinent to the explosive activity of Somma–Vesuvius, Campi Flegrei and Ischia Island, which were active in the investigated time span (e.g., [60–62]).

Somma–Vesuvius is formed by the Vesuvius cone (<2000 years) grown within a caldera dissecting an older (<40 ka) edifice, presently known as Mt. Somma. The Somma caldera is the result of four Plinian eruptions that dismantled and reshaped the old edifice during a poly-phased, caldera-forming stage [61,63]. The oldest of these Plinian events is the Pomici di Base eruption (22.03 ka, [64]; 22.47–21.68 ka, [65]), followed by the Mercato eruption (8.89 ka, [64]; 9.01–8.76 ka, [65]), the Avellino eruption (~3.9 ka, [66,67]) and, lastly, the famous 79 CE "Pompeii" eruption. The period between caldera-forming eruptions was punctuated by the Pomici Verdoline sub-Plinian eruption (19.27 ka, [64]; 19.37–19.16 ka [65]), and six sub-Plinian to Strombolian eruptions, named AP1 to AP6 (plus two minor intervening events named AP3α and AP4α), which occurred between the Avellino and 79 CE events [68,69]. The AP events are also known as protohistoric eruptions [70]. Following the 79 CE eruption, the renewal of the explosive to effusive activity within the caldera led to the formation of the Vesuvius cone, which last erupted in 1944 CE [61,71].

Campi Flegrei is a nested caldera [72,73] resulting from the Campanian Ignimbrite eruption (CI; 39.28 ka, [74]; 39.85 ka, [75]) and the Neapolitan Yellow Tuff eruption (NYT; 14.9 ka, [76]; 14.38–13.98 ka, [65]), though the oldest volcanic record in the Campi Flegrei area dates back to at least 110 ka [77]. The activity younger than ~15 ka, resulting from multiple vents, was clustered within the NYT caldera and grouped into three epochs of volcanism [78,79] totaling ~70 small to medium (and minor large) eruptions. Epoch I (15–10.6 ka) comprises at least 32 eruptions, Epoch II (9.6–9.1 ka) comprises 6 eruptions

and Epoch III (5.5–3.5 ka) comprises at least 27 eruptions. The last eruption occurred in 1538 CE, known as the Monte Nuovo eruption (e.g., [80,81]).

Ischia Island represents the emerged portion of a volcanic structure, rising from the seafloor in the Gulf of Naples, whose activity covers a >150 ka time span (e.g., [60,82]) characterized by explosive to effusive volcanism and volcano-tectonic processes. The largest event was the ~56 ka Monte Epomeo Green Tuff (MEGT) eruption, which resulted in a caldera collapse followed by block resurgence [60,83]. After the MEGT eruption, a new phase of intense volcanism (28–18 ka) was characterized by both explosive, magmatic to phreatomagmatic and Plinian-type eruptions, and effusive activity [60]. The last period of activity started about 10 ka bp and continued until the last eruption occurred in 1302 CE [84], known as the Arso eruption. About 46 eruptions occurred during this last phase of activity, resulting in lava flows and domes, scoria cones, tuff rings, tuff cones and widespread sheets of ash and pumice lapilli [84].

4. Geo-Volcanological Setting of Pompeii Archaeological Site

Ancient Pompeii was built on a hill, rising from the surrounding Sarno plain (Figure 1), that represents the remnant of local volcanic vents [31,85]. The volcanic activity resulted in both lava and pyroclastic deposits, representing the oldest volcanic rocks cropping out in Pompeii, and hereafter referred to as the "Pompeii bedrock" (i.e., the geological framework of the Pompeii hill). The Pompeii bedrock is cut seaward (south) by a paleocliff (Figure 1) formed during the early Holocene sea level rise [31,32,44,86], which occurred ~7 ka bp. The plain to the south of Pompeii, on the sea side (Figure 1), experienced paleoenvironmental changes associated with sea level variations, volcano-tectonic processes and aggradation of volcanic deposits, with the formation of shallow marine environments, dunal ridges and backridges and fluvial–marshy environments sealed by the 79 CE pyroclastic deposits (e.g., [31,32,44,86]). The Pompeii bedrock is well-exposed in the southern part of the archaeological site (Insula Meridionalis, Figure 2), where it forms a sub-vertical scarp resulting from anthropogenic modifications and quarrying activity along the paleocliff [31]. Scattered outcrops of the Pompeii bedrock also occur in the western part of the city (Insula Occidentalis, Figure 2) and within the archaeological site, as in insula 2 of Regio I or at the base of the Amphitheatre (Regio II). From a geochemical point of view, lava samples collected from Insula Meridionalis and at the Amphitheatre have been classified as leucite-bearing tephrite by Di Girolamo [87,88]. More recently, Kastenmeier et al. [89] classified the Pompeii lavas as shoshonite. These rocks, as well as pyroclastic and sedimentary deposits from the surrounding area, were extensively used as row materials for buildings and mortars [89–92]. Based on the macroscopic characteristics, Amato et al. [31] divided the lava sequence into a basal unfractured, dark gray, porphyritic unit (unit A) with phenocrysts of leucite and clinopyroxene, representing most of the thickness, an intermediate weakly fractured unit (unit B) and an upper extremely weathered unit (unit C) consisting of a reddish, scoriaceous, leucite-rich foam. The age of the Pompeii bedrock is not well-constrained. Cinque and Irollo [85] reported a paleosol, containing pumice fragments attributed to the Mercato eruption, on top of the Pompeii bedrock near Porta Vesuvio (Figure 2), suggesting a relative age older than ~9 ka. Rolandi et al. [93] suggested a much older relative age as they reported a pumice layer, speculatively attributed to the 22 ka Pomici di Base eruption (referred to as the "Sarno eruption" by the authors), on top of lavas in an excavation near Porta Nocera (Figure 2). A similar relative age (>18–20 ka) is provided by Di Vito et al. [94] based on radiocarbon determinations on two paleosols underlying two lava bodies cored to the south of Pompeii. Regarding the lower limit, borehole data [85,94,95] suggest that the Pompeii bedrock postdates the ~40 ka Campanian Ignimbrite eruption, the largest explosive event sourced from Campi Flegrei, whose ignimbrite deposits blanketed the

whole Campania region [96–100]. In addition, Rittmann [101] reported a pumice layer underlying a lava body in a well dug in 1931 in the Casa dei Vasi di Vetro (Vas in Figure 2). This pumice layer was speculatively attributed by Rolandi et al. [93] to the Codola eruption (~33 ka, [102]; 33.96–32.63 ka, [65]), whose source area is unclear and has been attributed to either Somma–Vesuvius or Campi Flegrei (e.g., [102,103]).

The Pompeii bedrock is covered by a sequence of loose to compacted sediments consisting of primary tephra layers, reworked volcaniclastic deposits, buried soils and anthropogenic deposits. The total thickness of the sediments is variable due to anthropic activity and the uneven surface of the Pompeii bedrock, ranging from absent (outcropping bedrock) to a few meters [31]. The stratigraphic and geotechnical features of the terrains, sandwiched between the Pompeii bedrock and the 79 CE street level, were investigated through six drillholes in the Insula dei Casti Amanti (Figure 2), reaching depths between 13 and 25 m [104]. Marturano et al. [45] arranged the pre-79 CE cored sequence, drilled in the Insula dei Casti Amanti, in three decimeter- to meter-thick units (labeled "layer") resting on the lavas of the Pompeii bedrock (layer 4). From the bottom upwards, Marturano et al. [45] recognized the following:

- Layer 3: dark brown, volcanic silty sands without artifacts.
- Layer 2: a volcanic sandy deposit changing upward in color from brown-yellowish to gray. It is rich in pumice clasts at the bottom. Pumice fragments have been attributed to the Mercato eruption based on the geochemical signature. This layer contains material fragments belonging to the late Neolithic Diana culture. In addition, the authors report the occurrence of scant fossil remains associated with shallow marine environments, suggesting an uplift of the Pompeii area by up to 30 m in the last 6000 years.
- Layer 1: anthropic layers, rich in pottery fragments and bricks, between street levels dated from III century BCE to 79 CE.

A yellowish volcaniclastic layer attributed to the Mercato eruption, covered by a dark paleosol containing light-colored pumice and material fragments of the late Neolithic Diana culture, was also found in four archaeological trenches dug along the alleys of the same insula, in early 2000 [29,105,106].

Regarding the sequence younger than the Mercato eruption, Robinson [50] reported a composite stratigraphy consisting of at least four tephra layers separated by paleosols found in trenches in the area between Porta Vesuvio and Regio V (Figure 2). Tephra layers were attributed to all Neapolitan volcanoes based on the radiocarbon ages of the organic findings and tephrochronological data: the lowest two were attributed to Campi Flegrei (likely from the Astroni sequence, ~4 ka [78,79]), one tephra was attributed to Vesuvius (an AP eruption) and the uppermost to Ischia (likely Cannavale tephra, 2.9 ka [84]). Tephra layers attributed to Campi Flegrei and Somma–Vesuvius are separated by soils containing pottery fragments of the EBA Palma Campania culture. Moreover, Ranieri [48] reported four tephra layers, in trenches in the area of the so-called Porta Capua (PC in Figure 2), speculatively attributed to the Mercato eruption and at least three AP eruptions.

Recently, Amato [51] provided a more detailed geoarchaeological framework of the sediments on top of the Pompeii bedrock. The author described three superimposed macro-units consisting of tephra layers, volcaniclastic reworked sediments and buried soils belonging, respectively, to the Upper Paleolithic, Neolithic and Protohistoric period. The Upper Paleolithic unit consists of loose, brown, volcaniclastic silty sands containing organic matter. This unit includes three primary to partly reworked volcanic horizons grading upward into paleosols. The Neolithic Unit consists of a dark-brown silty to sandy paleosol, rich in organic matter, containing white pumice fragments whose amount increases towards the base. The pumice clasts are similar to those attributed to the Mercato eruption by Marturano et al. [45]. The finding of material fragments of the Diana culture

allowed this paleosol to be dated to the (late) Neolithic. The Protohistoric Unit consists of sandy volcaniclastic deposits and poorly developed paleosols. At least three volcanic layers, composed of ash and fine lapilli horizons, are included in this unit and tentatively attributed to the protohistoric activity of Somma–Vesuvius.

5. Materials and Methods

As part of the archaeological investigations preparatory to the installation of the new roofing system [59], twelve trenches were dug, down to ~4 m of depth below the 79 CE street level, along the alleys that flank the Insula dei Casti Amanti (Figure 2), providing the unique opportunity to carry out a thorough stratigraphic survey of the pre-79 CE stratigraphic sequence based on a number of trenches. Trenches CA1 to CA6 are located along the east alley, while trenches CA7 to CA12 are located along the west alley (Figure 2). The geoarchaeological stratigraphy provided by Amato [51] serves as the basic chronostratigraphic framework for describing all the pre-79 CE tephra layers on top of the Pompeii bedrock. The structure of each tephra layer and the textural and lithologic characteristics of the juvenile fragments have been described in detail. Based on these characteristics, tephra layers have been laterally correlated in order to provide a composite pre-79 CE volcanic stratigraphy at Pompeii. The tephra layer attributed to the Mercato eruption by Marturano [45], which is well-recognizable at the base of the Neolithic Unit in all trenches, has been considered a (chrono)stratigraphic marker against which the stratigraphic position of the other tephra layers has been identified. Samples have been collected from all tephra horizons. Grain size analyses have been performed on selected samples collected from well-preserved tephra layers. Samples have been oven-dried and mechanically sieved, at 1Φ intervals, down to 4Φ (0.063 mm) in order to calculate the grain size parameters according to Folk and Ward [107]. Bulk rock chemical analysis has been performed on juvenile fragments by Inductively Coupled Plasma-Mass Spectrometry (ICP-MS). We have identified the most reliable source eruption and age of each tephra layer by (1) comparing the chemical composition of the juvenile fragments to that of the products of late Pleistocene to Holocene explosive eruptions vented from Neapolitan volcanoes, and (2) considering the relative stratigraphic position of each tephra layer with respect to the Mercato tephra. The stratigraphic framework of the tephra layers, where well-preserved, helped in the attribution to specific eruptions. In addition, following the textural characterization of the lavas provided by Amato et al. [31], a macroscopic textural characterization of the pyroclastic deposits of the Pompeii bedrock, cropping out in the Insula Meridionalis, has been performed.

6. Results

The description of the pre-79 CE sequence at Pompeii, reported in the next sections, follows a timeline from the Pompeii bedrock (Figure 3) to the overlying units (Figure 4). The investigated stratigraphic sequence (Figure 4a) rests on a gray, weakly fractured, leucite-bearing lava (unit B of Amato et al. [31]) whose top is extremely weathered and orange to reddish in color. This lava (Figure 4b) has been intercepted only in trenches positioned in the southern sector of the insula, close to via dell'Abbondanza (trenches CA1 and CA2 in the east alley, trenches CA7 and CA8 in the west alley, Figure 2), indicating a general northward dip. This is consistent with the presence of a morphological depression, as already suggested by previous authors [57,58,104], who provided a cross-section, through borehole data, of the subsoil profile along the alleys. This basin-like morphology of the Pompeii bedrock, beneath the insula dei Casti Amanti, has favored the accumulation and thickening of sediments. Due to these morphological features and the thickening of the cover terrains, the lowermost pyroclastic units have not been intercepted in northernmost

trenches. Anthropogenic cuts and infills and street levels (Figure 4c) constitute the uppermost layers in all trenches [51]. The pre-79 CE composite stratigraphy includes at least eight tephra layers (Figure 5), labeled progressively from TL1 (oldest) to TL8 (youngest). Three tephra layers (TL1 to TL3) have been recognized in the Upper Paleolithic unit, one tephra layer (TL4) in the Neolithic unit and four (TL5 to TL8) in the Protohistoric unit. The bulk rock chemical data acquired for each tephra, reported in Table 1, as well as the compositional fields of the correlated products from the literature data are plotted in the Total Alkali vs. Silica diagram (TAS, [108]; Figure 6) and selected binary diagrams (Figure 7). Sedimentological data of selected samples are reported in Table 2.

Table 1. Major (wt.%) and trace (ppm) elements of juvenile samples collected from pre-79 CE tephra layers at Pompeii. Major elements are recalculated to 100% water-free. Loss on ignition (L.O.I.) values are reported. TL1p and TL1sc represent, respectively, pumice and scoria clasts of unit TL1.

	Tephra Layers (Samples)								
	TL1p	**TL1sc**	**TL2**	**TL3**	**TL4**	**TL5**	**TL6**	**TL7**	**TL8**
SiO_2	60.40	53.79	60.82	58.53	59.17	55.08	54.01	52.24	52.64
Al_2O_3	18.16	18.32	18.93	19.56	21.59	18.72	18.66	18.51	19.33
Fe_2O_3	3.61	7.87	3.79	5.43	2.25	5.67	5.98	6.67	6.77
MnO	0.15	0.15	0.14	0.14	0.18	0.14	0.14	0.14	0.15
MgO	0.50	2.21	0.76	1.34	0.21	2.92	3.48	3.34	2.57
CaO	5.22	7.87	2.28	3.44	2.01	6.09	6.55	8.08	7.34
Na_2O	3.96	3.02	4.32	3.01	7.56	3.95	3.23	3.48	3.37
K_2O	7.64	5.58	8.17	7.81	6.87	6.31	6.81	6.25	6.59
TiO_2	0.35	0.74	0.44	0.57	0.15	0.65	0.67	0.79	0.74
P_2O_5	b.d.l.	0.46	0.36	0.17	b.d.l.	0.46	0.45	0.50	0.50
L.O.I.	4.00	1.21	2.87	3.86	8.34	3.12	4.18	4.93	5.76
As	15.2	9.03	16.8	14.4	46.8	17.4	13.5	10.8	11.6
Ba	375	1513	321	1513	85.8	1151	1291	1450	1518
Be	10.9	7.54	9.25	10.1	31.3	10.0	9.28	8.57	9.18
Bi	0.24	0.10	0.39	0.37	0.85	0.37	0.26	0.19	0.21
Cd	0.15	0.12	0.13	0.16	0.14	0.18	0.15	0.11	0.12
Co	2.05	14.6	3.00	6.74	0.79	16.5	14.6	17.7	16.3
Cr	6.0	9.6	5.1	25.0	3.5	53.5	72.4	46.8	30.3
Cs	18.4	12.9	25.8	28.0	56.7	18.4	22.5	15.9	19.1
Cu	4.0	15.4	3.6	8.1	2.1	37.5	51.8	31.7	24.5
Ga	18.7	20.2	18.2	19.3	29.9	19.4	19.3	19.1	19.6
Ge	1.58	1.60	1.48	1.66	1.50	1.49	1.47	1.40	1.42
Hf	7.87	5.60	6.99	6.77	14.2	6.21	5.75	5.57	5.64
In	0.04	0.05	0.04	0.04	b.d.l.	0.04	0.04	0.04	0.04
Mo	4.59	2.89	3.34	3.34	4.69	2.26	2.39	2.98	2.76
Nb	46.1	30.3	42.4	40.1	88.9	42.7	41.2	37.9	39.8
Ni	2.6	4.4	b.d.l.	5.7	b.d.l.	83.0	24.6	19.0	12.4
Pb	52.2	34.7	45.0	47.3	110	46.8	48.9	41.9	44.1
Rb	294	264	357	299	497	250	265	269	320
Sb	0.67	0.41	1.34	0.84	1.90	0.86	0.94	0.62	0.66
Sc	2.18	10.95	3.21	5.55	0.63	12.10	14.76	15.75	10.70
Sn	4.03	3.61	3.72	3.88	4.71	3.38	3.17	3.32	3.50
Sr	463	979	289	630	71.9	662	755	866	926
Ta	3.09	2.01	2.74	2.56	2.98	2.37	2.17	2.06	2.21
Th	30.7	19.5	28.7	28.3	83.7	27.9	29.0	25.1	26.1
U	8.84	5.52	7.45	6.34	30.7	6.97	8.01	7.43	7.39
V	19.2	154	52.2	83.8	14.0	120	139	172	164
W	7.60	4.50	6.55	5.92	12.4	5.38	5.97	4.98	5.98
Y	32.1	28.2	25.0	30.5	13.9	22.6	22.3	23.0	22.2

Table 1. *Cont.*

	Tephra Layers (Samples)								
	TL1p	**TL1sc**	**TL2**	**TL3**	**TL4**	**TL5**	**TL6**	**TL7**	**TL8**
Zn	87.0	93.3	75.6	82.1	145	92.1	82.9	77.6	82.2
Zr	357	238	316	303	786	296	274	254	267
La	66.5	52.6	61.9	69.0	93.7	61.1	67.3	62.0	61.4
Ce	134	108	123	129	164	114	127	122	122
Pr	13.9	12.4	12.7	14.8	14.9	12.2	13.0	13.0	12.6
Nd	48.9	47.1	43.6	53.0	42.2	42.9	45.3	46.8	45.0
Sm	9.04	9.27	7.79	9.86	5.04	7.71	8.14	8.73	8.31
Eu	1.87	2.23	1.63	2.31	0.639	1.76	1.86	2.06	1.97
Gd	6.90	7.22	5.87	7.52	3.15	5.85	6.13	6.53	6.17
Tb	1.02	1.01	0.886	1.08	0.405	0.821	0.835	0.892	0.852
Dy	5.82	5.54	5.04	5.96	2.22	4.51	4.45	4.76	4.60
Ho	1.15	1.06	0.965	1.13	0.438	0.852	0.824	0.872	0.845
Er	3.17	2.73	2.58	2.99	1.26	2.25	2.15	2.25	2.18
Tm	0.476	0.400	0.391	0.439	0.209	0.327	0.309	0.324	0.314
Yb	3.12	2.49	2.53	2.82	1.55	2.08	1.96	2.02	1.97
Lu	0.485	0.388	0.380	0.429	0.243	0.320	0.294	0.298	0.298

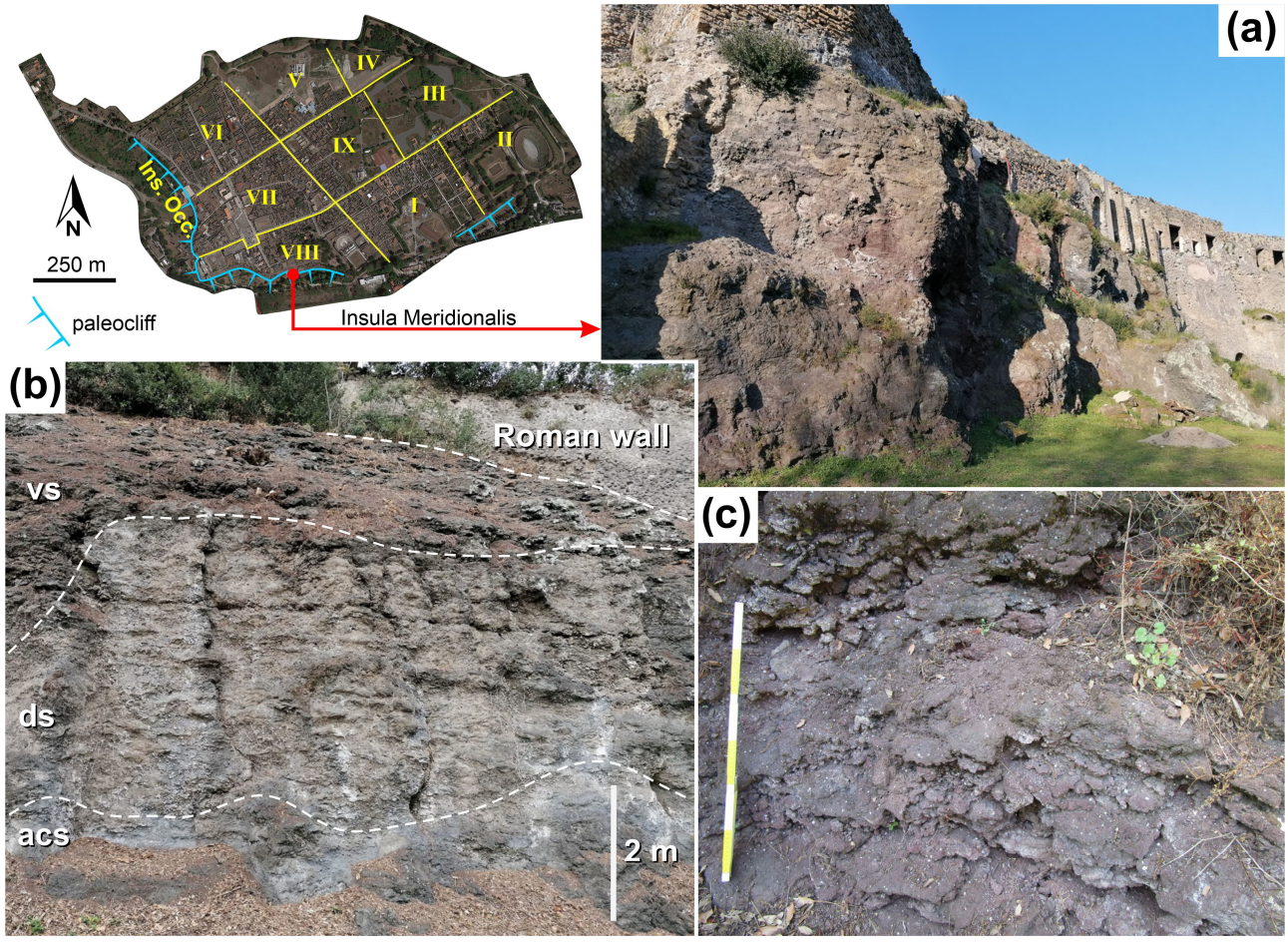

Figure 3. Insula Meridionalis: (**a**) panoramic view of the sub-vertical scarp (paleocliff) consisting mainly of welded spatter deposits (note the Roman structures built on top of the scarp); (**b**) typical vertical lithofacies variation in welded deposits from apparently coherent spatter (acs), through dense spatter (ds), to vuggy spatter (vs); this lithofacies classification [109] has been also used to describe spatter products erupted from lateral vents at Somma–Vesuvius [110]; (**c**) close-up view of the poorly welded to unwelded vuggy spatter lithofacies in the upper part of the scarp. Inset: plan view of Pompeii archaeological site with contour of the paleocliff.

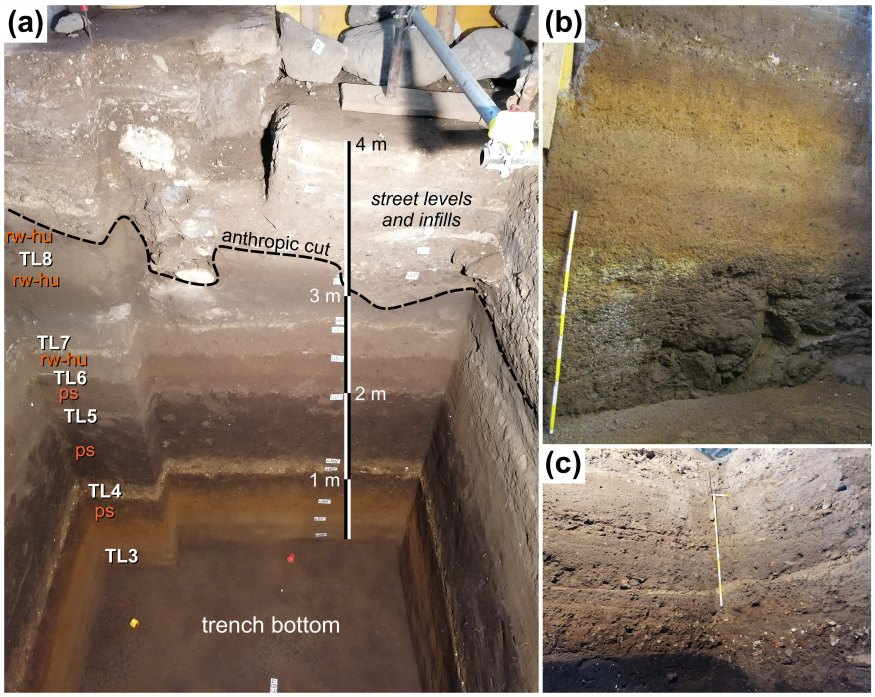

Figure 4. Insula dei Casti Amanti: (**a**) view (from above) of the northern wall of trench CA6 showing six (out of eight) superimposed tephra layers (TLs) separated by light to dark brown paleosols (ps) and reworked and humified (rw-hu) volcaniclastic deposits. The upper part of the sequence is truncated by anthropic cuts and infills and street levels; (**b**) detail of the lava (unit B of Amato et al. [31]) underlying the investigated stratigraphic sequence (trench CA7); (**c**) detail of the streel levels and infills (III century BCE–79 CE) cutting through the upper part of the sequence (trench CA4).

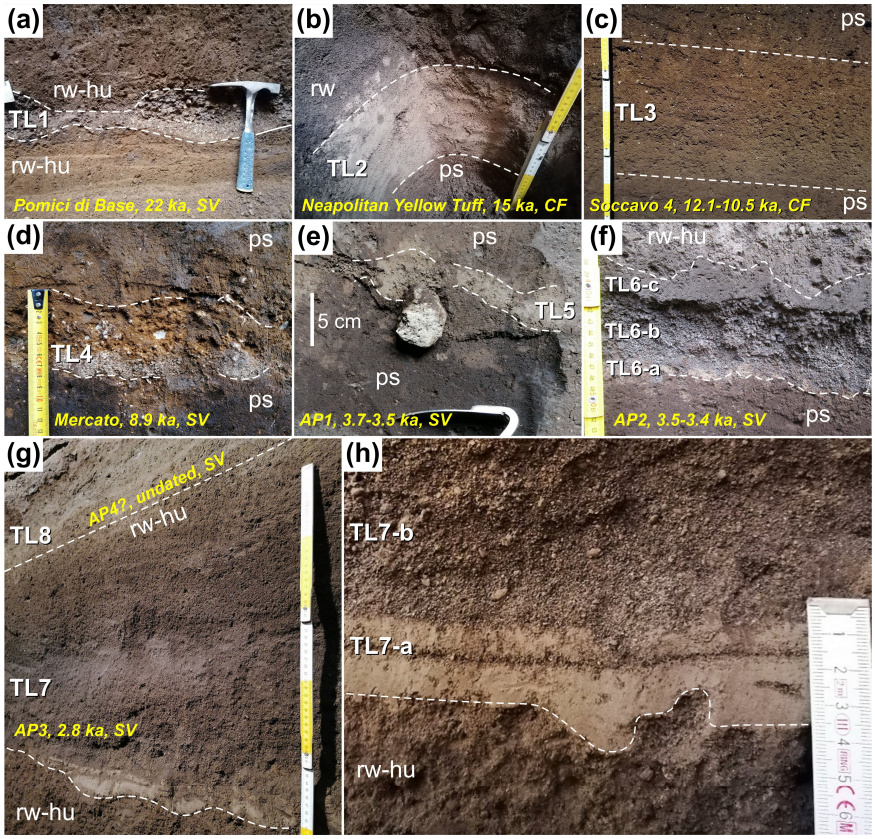

Figure 5. Photos of tephra layers (TL1 to TL8) sandwiched between the Pompeii bedrock and the 79 CE street level in the investigated trenches at Pompeii. (**a**–**c**) Upper Paleolithic unit tephra;

(**d**) Neolithic unit tephra; (**e**–**h**) Protohistoric unit tephra. The eruption, age and source area are reported for each tephra: SV = Somma–Vesuvius. CF = Campi Flegrei. Note the ballistic pumice fragment deforming the ash of TL5. Intervening materials are labeled as follows: rw = reworked; hu = humified; ps = paleosol. Question mark (?) indicates uncertain attribution.

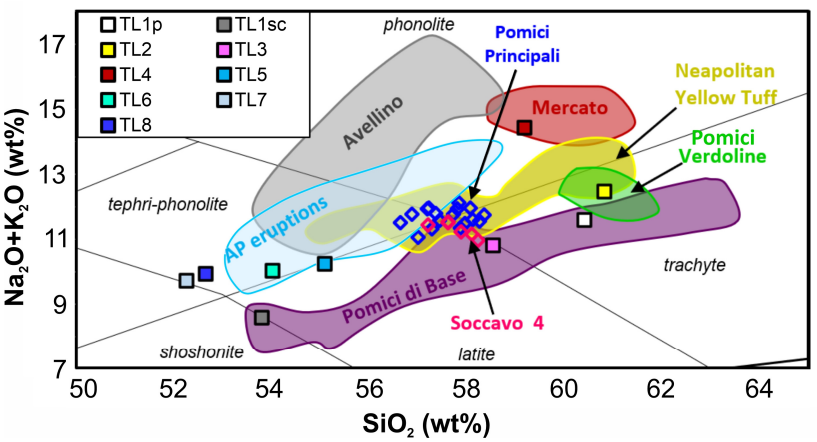

Figure 6. Total Alkali vs. Silica classification diagram for bulk rock compositions of the investigated tephra layers. Sources of data: Pomici di Base eruption [64,111–113]; Pomici Verdoline eruption and AP eruptions group [64]; Neapolitan Yellow Tuff eruption [114–116]; Mercato eruption [45,64,112,117]: Pomici Principali eruption [118–120]: Soccavo 4 eruption [118,119]; Avellino eruption [64,112,121,122].

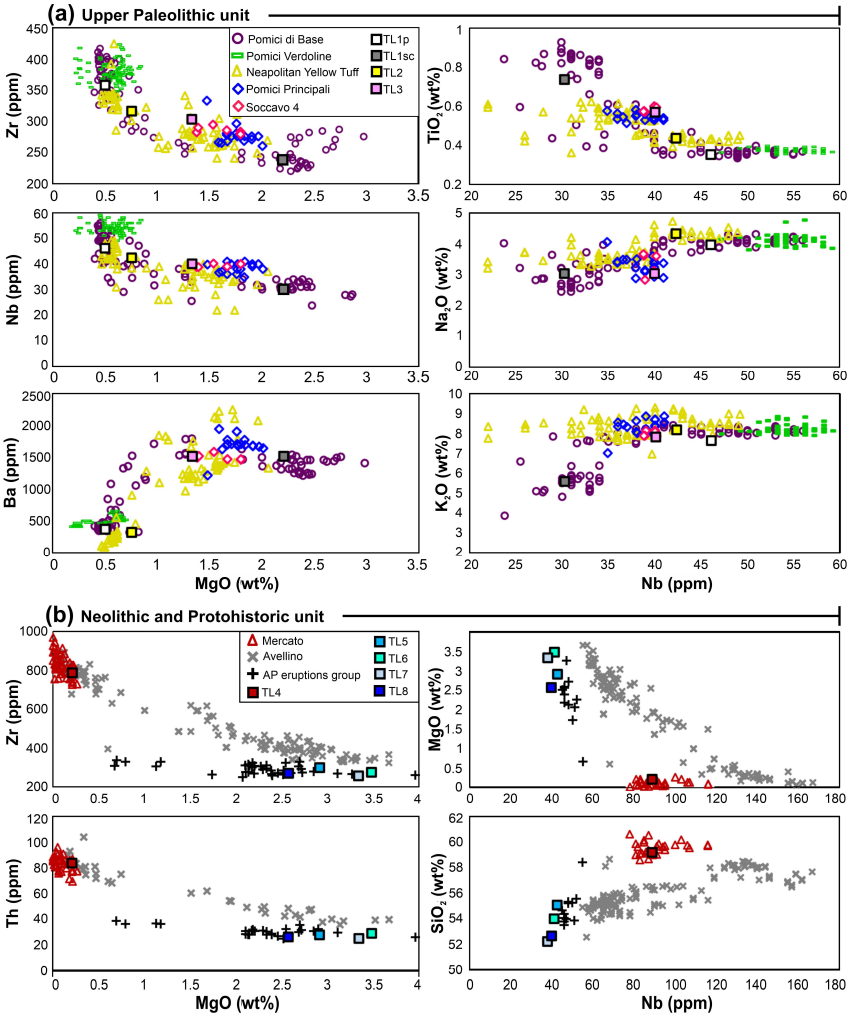

Figure 7. Selected major vs. trace element diagrams for the investigated tephra layers: (**a**) Upper Paleolithic unit and (**b**) Neolithic and Protohistoric unit. Sources of literature data as in Figure 6.

Table 2. Sedimentological data of selected samples from well-preserved tephra layers (TL6 and TL7) and correlation with the stratigraphic scheme (*) of the AP eruptions of Andronico and Cioni [69].

Sample	Eruption	Mean (Mz)	Median (Md_Φ)	Sorting (σ_Φ)	Skewness	Kurtosis	F1 wt.% < 1 mm	F2 wt.% < 0.063 mm
CA6/TL7b_top	AP3 (bed B *)	0.77	0.75	1.16	0.10	1.17	77.52	3.19
CA6/TL7b_base	AP3 (bed B *)	0.74	0.72	1.19	0.09	1.18	75.81	2.79
VM/TL6b_top	AP2 (bed C *)	−0.94	−1.00	1.33	0.16	1.33	20.13	1.12
VM/TL6b_base	AP2 (bed C *)	−0.26	−0.28	1.21	0.13	1.27	40.28	1.48

6.1. The Pyroclastic Deposits of the Pompeii Bedrock

The macroscopic textural characteristics of the pyroclastic deposits of the Pompeii bedrock have been studied in the southernmost part of the archaeological site (Insula Meridionalis, Figure 3), the only area where an extensive exposure (about 200 m long) of the volcanic rocks along the paleocliff is available, allowing direct observations. The scarp is up to 13–15 m high (Figure 3a). The base of the sequence does not crop out. Roman structures are built directly on top of the scarp (Figure 3a). Here, the Pompeii bedrock is predominantly made up of clastic deposits, locally reddened, consisting of coarse, centimeter- to decimeter-sized, leucite-bearing (phenocrysts) scoriaceous to spatter (fluidal and incandescent magma rags) fragments, showing a variable degree of welding. Centimeter-sized clasts are roughly equant in shape, while decimeter-sized clasts show flattened morphologies whose aspect ratio (major axis/minor axis) is up to 5:1.

The macroscopic textural description of the welded spatter deposits follows the classification proposed by Carracedo Sánchez et al. [109], who defined three lithofacies characterized by a different degree of welding: (1) *vuggy spatter*, where clasts are welded only at contact points or small areas (agglutination), clast contours are clearly discernible and the deposit is formed by a clastic aggregate with abundant voids; (2) *dense spatter*, where clasts are agglutinated along most of the contact surface, clast contours are locally discernible and the deposit is a clastic aggregate with rare voids; (3) *apparently coherent spatter*, where clasts are coalesced along whole contact surfaces and clast outlines are unclear. This lithofacies classification was also applied to pre-caldera (>22 ka) scoria- and spatter-cones at Somma–Vesuvius [110]. Overall, in the study area, spatter deposits show a superimposition of lithofacies reflecting a progressive decrease in the degree of welding, transitioning from apparently coherent spatter at the base, through dense spatter in the middle, to vuggy spatter at the top (Figure 3b,c). Most of the visible thickness (7–8 m on average) consists of dense spatter, forming a well-developed layering gently dipping to the S-SE, while the other two lithofacies are 3 m thick on average. The upward transition from apparently coherent spatter to dense spatter appears smooth, while the subsequent upward transition to vuggy spatter is sharp. Moving laterally along the scarp, the same superimposition of lithofacies is observed although thickness variations have been recognized.

6.2. Upper Paleolithic Unit

The lowermost tephra layer (TL1, Figure 5a) rests on top of a lava (Pompeii bedrock) via interposition of a sandy, reddish to brownish, reworked and weakly humified deposit, up to 25 cm thick, containing leucite-bearing lava fragments deriving from the weathering of the underlying lava. TL1 consists of lenses of medium to coarse, sub-angular, slightly porphyritic to sub-aphyric lapilli overlying a thin (1 cm), gray, indurated, fine ash layer. Lenses of lapilli are up to 10 cm thick and 50 cm long. Sporadic mm-sized lava fragments are dispersed. Juvenile fragments are predominantly light gray, well vesiculated, slightly porphyritic (feldspar and pyroxene) pumice, whilst a minor fraction is made up of dark gray, moderately vesiculated, sub-aphyric scoria clasts. Some pumice clasts show a brownish

patina, and a low amount of brownish matrix locally fills the inter-granular voids due to reworking. This tephra has been recognized only in two trenches (CA3 and CA8, Figure 2). TL1 is covered by a sandy to silty, grayish to brownish, 30–50 cm thick, reworked volcaniclastic deposit containing gray pumice fragments, grading upward in a 25 cm thick, brown paleosol. Fresh, light gray pumice (sample TL1p) and dark gray scoria fragments (sample TL1sc) have been analyzed separately. Compositionally, pumice fragments show an evolved composition (SiO_2 = 60.4 wt.%, alkali sum = 11.6 wt.%) and fall in the field of trachyte, while dark gray fragments are less evolved (SiO_2 = 53.8 wt.%, alkali sum = 8.6 wt.%) and straddle the boundary between latite and shoshonite (Figure 6). The recognition in TL1 of pumice to scoria juvenile types, with a trachytic to latitic/shoshonitic composition, is fully consistent with the attribution of TL1 to the 22 ka Pomici di Base eruption [64,111,112], the largest Plinian event of Somma–Vesuvius [113]. The Pomici di Base fall deposit consists of a basal white pumice lapilli bed, an intermediate transitional bed of gray pumice lapilli and an upper scoria lapilli bed [113]. Compositionally, the Plinian fall deposit is zoned, showing a continuous vertical gradient from trachyte to latite, as follows [111]: most evolved trachyte (trachyte "a", MgO ≈ 0.45–0.5 wt.%) forms the base of the white pumice bed; less evolved trachyte (trachyte "b", MgO ≈ 0.5–1 wt.%) forms the upper part of the white pumice bed and the lower part of the transitional bed; most evolved latite (latite "a", MgO ≈ 1–1.3 wt.%) forms the upper part of the transitional bed; less evolved latite (latite "b", MgO ≈ 1.8–2.4 wt.%) forms the upper scoria bed. Light gray pumice clasts from TL1 have MgO = 0.5 wt.% (sample TL1p, Figure 7a) at the boundary between Trachyte "a" and Trachyte "b", while dark scoria fragments have MgO = 2.2 (sample TL1sc, Figure 7a) compatible with Latite "b", confirming the attribution of TL1 to the Pomici di Base eruption. The thin ash layer and the overlying lapilli represent, respectively, units U-1 and U-2 (c to d) of Bertagnini et al. [113] and record the opening phase and part of the Plinian fallout of the eruption.

TL2 (Figure 5b) is a light gray/whitish, compacted, fine ash containing light gray, sub-aphyric (biotite), fine pumice lapilli. In most trenches, it appears as a reworked grayish–whitish ash, locally identifiable as thin lenses. It shows evidence of primary deposition only in trench CA9 (Figure 2), where it is a 20 cm thick. It is compacted to cohesive, massive, light gray ash (Figure 5b) capped by a decimeter-thick, volcaniclastic, reworked deposit culminating in a 40 cm thick, dark brown paleosol. This paleosol embeds, in the upper half, pale gray haloes or patches of humified grayish ash associated with a separate, barely distinguishable tephra. Juvenile clasts from TL2 are trachytic in composition (SiO_2 = 60.8 wt.%, alkali sum = 12.5 wt.%) when plotted on the TAS diagram (Figure 6). At first glance, the TL2 composition is consistent with the compositional field of the 19.3 ka Pomici Verdoline sub-Plinian eruption. The products of the Pomici Verdoline eruption are characterized by a very homogeneous trachytic composition and a narrow variability of both major and trace elements [64,123]. By plotting selected major and trace elements, it appears clear that TL2 is outside the narrow compositional field of the Pomici Verdoline eruption (Figure 7a), showing a much more consistent chemical affinity with the 15 ka NYT eruption [114–116], the second largest caldera-forming event of Campi Flegrei [72,73,124], which represents the best candidate for the correlation of this tephra.

TL3 (Figure 5c) is an ash layer containing well-vesiculated, slightly porphyritic (feldspar), gray, fine pumice lapilli and rare sub-millimeter-sized lithic lava fragments. It varies in color from gray at the base to orange at the top due to weathering. The thickness ranges from 35 to 50 cm, although it must not be considered as a primary thickness as it is influenced by abundant reworking, causing overthickening. The orange part passes upward in a 40–50 cm thick brown paleosol, the uppermost of the Upper Paleolithic unit, containing gray pumice fragments. The sample from TL3 (Figure 6) falls in the field of latite at the boundary with trachyte (SiO_2 = 58.5 wt.%, alkali sum = 10.8 wt.%). Its stratigraphic

position, above the 15 ka NYT tephra (unit TL2) and beneath the 8.9 ka Mercato tephra (unit TL4), allows us to exclude TL3 having been sourced from Somma–Vesuvius or Ischia. Indeed, in this ~6000-year-long time span (~15–9 ka), Somma–Vesuvius was dormant and tephra layers found on Mt. Somma slopes have been attributed to the activity of Campi Flegrei [61,64]. Similarly, Ischia has been mostly quiescent and produced effusive eruptions, with the formation of lava domes and lava flows around 10 ka bp [84]. Conversely, the Campi Flegrei caldera was very active in the ~15–9 ka period and produced at least 38 eruptions in the first two epochs of activity [78,79]. Among these, the Pomici Principali eruption (12.1–11.9 ka [79]) and the Soccavo 4 eruption (12.1–10.5 ka [79]), whose products were dispersed over large areas (e.g., [125,126]), show largely overlapping compositions [118–120] similar to TL3 (Figure 6). However, binary diagrams (Figure 7a) show a slightly better correlation with the Soccavo 4 eruption.

6.3. Neolithic Unit

TL4 (Figure 5d) appears as a yellow to orange, reworked ash containing abundant white, well-vesiculated, aphyric to sub-aphyric, sub-angular, fine to coarse pumice lapilli. The amount of lapilli decreases upward. Lenses or pockets of white pumice lapilli, up to 3.5 cm thick and 30 cm long, preserved in the underlying paleosol, represent remnants of the primary deposit. This tephra is covered by a very dark brown to blackish, sandy to silty paleosol, rich in organic matter (with the highest degree of pedogenesis among all the buried soils), up to 90 cm thick, containing mm- to cm-sized white pumice fragments and abundant rhizoconcretions (vertical elongate concretion-like structures formed around roots). TL4 also occurs as an alignment of coarse pumice fragments (maximum diameter up to 8 cm) at the interface between two paleosols. The sample from TL4 (Figure 6) is phonolitic in composition (SiO_2 = 59.2 wt.%, alkali sum = 14.4 wt.%) with a very low MgO content (0.21 wt.%) and high content of Al_2O_3 (21.6 wt.%) and Zr (786 ppm). Major and trace element plots (Figure 7b) show a clear attribution to the 8.9 ka Mercato eruption, as already determined by Marturano et al. [45]. The products of the Mercato eruption, dispersed towards the east, possess a nearly homogeneous phonolitic composition [64,112,117] and consist mainly of Plinian fall deposits, made up of well-vesiculated, aphyric to sub-aphyric, white to green–gray pumice, separated by ashfall layers and pyroclastic current deposits [127]. The textural characteristics of the pumice fragments of TL4 perfectly match those of the Mercato eruption. The finding of the primary deposits of the Mercato eruption in the form of small pockets of pumice lapilli, which survived erosion and reworking, suggests that this unit spans from the late Mesolithic (Mercato eruption) to the late Neolithic (paleosol bearing fragments of the Diana culture).

6.4. Protohistoric Unit

TL5 (Figure 5e) occurs as a discontinuous horizon or lenses of pale gray fine ash with sporadic accretionary lapilli, resting on the Neolithic paleosol (Figure 8). Locally, very small pockets of pale gray, fine pumice lapilli directly overlie the ash. Traces of bioturbation characterize this unit and extend down to 35 cm in the underlying paleosol. In trench CA11 (Figure 2), a pale gray, slightly porphyritic (feldspar and biotite), moderately vesiculated pumice fragment, 6 cm in diameter, ballistically emplaced, was found in this unit. It forms a small impact sag that deforms the ash, which is recognizable as very small pockets in the paleosol, just below the fragment (Figure 5e). In most cases, this unit is recognizable just as pale gray–whitish halos. TL5 passes upward in a 30–35 cm thick, light brown, sandy to silty paleosol (Figure 8) containing pale gray pumice fragments. The surface of this paleosol is slightly undulated, with wave heights of a few centimeters.

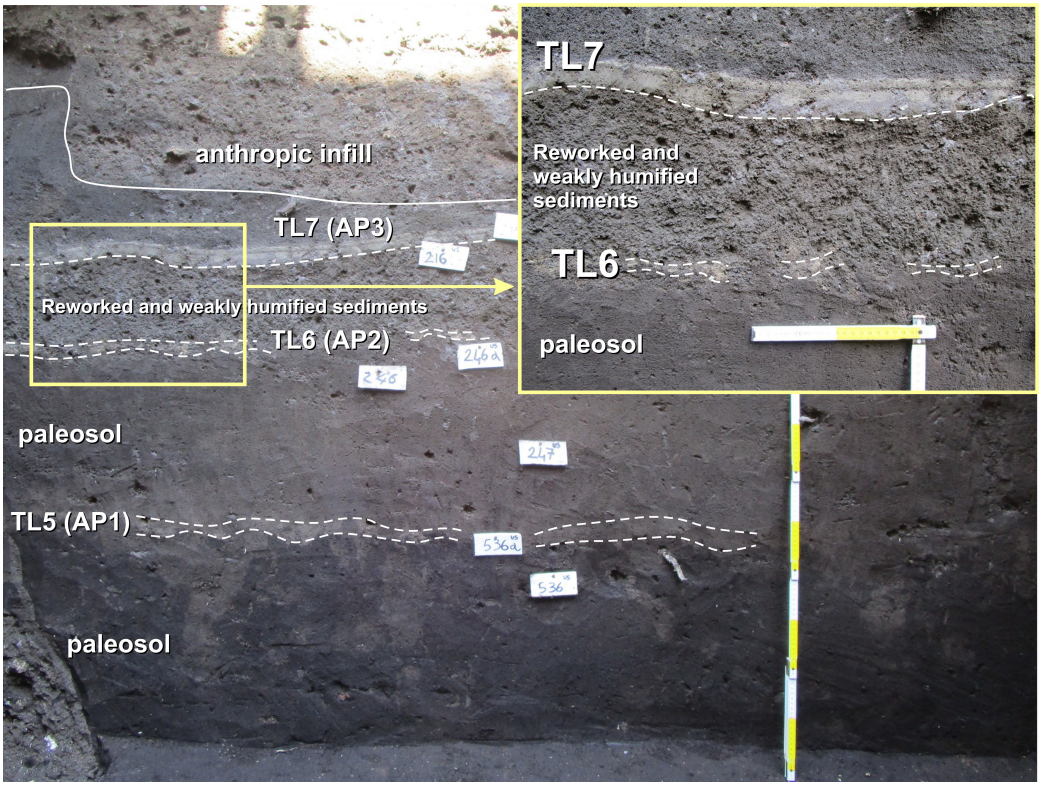

Figure 8. Tephra layers of the Protohistoric unit in the Insula dei Casti Amanti (trench CA12). The top of TL7 is truncated by an anthropic cut (white continuous line). The source eruption of each tephra is reported in parentheses. Inset: Close-up view of the reworked and weakly humified sediments between TL6 and TL7.

TL6 (Figure 5f) rests on the underlying paleosol and consists of three stratigraphic units (TL6-a, TL6-b and TL6-c): TL6-a is a 1.5–2 cm thick, very light-colored to pale yellow horizon of coarse pomiceous ash while TL6-b is a 9–10 cm thick, clast-supported, reverse-graded layer consisting of dark gray, poorly to micro-vesiculated, porphyritic (pyroxene and biotite) scoria lapilli and sporadic lithic lava fragments. Rare lighter-colored, moderately vesiculated (pomiceous) juvenile clasts are present; TL6-c is a grayish to greenish, massive, accretionary lapilli-bearing ash layer, up to 7–8 cm thick. In the Insula dei Casti Amanti, the basal coarse ash (TL6-a) occurs as a discontinuous horizon (Figure 8), the overlying stratigraphic units are deeply eroded and only very small pockets of fine lapilli (TL6-b) are recognizable. The stratigraphic framework of this tephra is well-preserved in trench VM (Figure 9) as well as in trench S16. Sedimentological analyses on two samples collected in trench VM, at the base (VM/TL6b_base) and at the top (VM/TL6b_top) of the gray lapilli, confirm that this sub-unit is reverse-graded and well sorted (Table 2). The median diameter varies upward from -0.28 to -1.0φ while the sorting coefficient is quite constant (1.21 at the base and 1.33 at the top). No paleosol has been found on top of TL6 in any trench. In the Insula dei Casti Amanti, as well as in trench S16, TL6 is capped by a reworked and weakly humified volcaniclastic deposit, 25–30 cm thick (Figure 8). In trench VM (Figure 9), the top of the upper ash layer (TL6-c) features an undulated surface, due to sub-aerial erosion, covered by a gray/greenish reworked ash, 3–4 cm thick, with no clear evidence of pedogenetic processes.

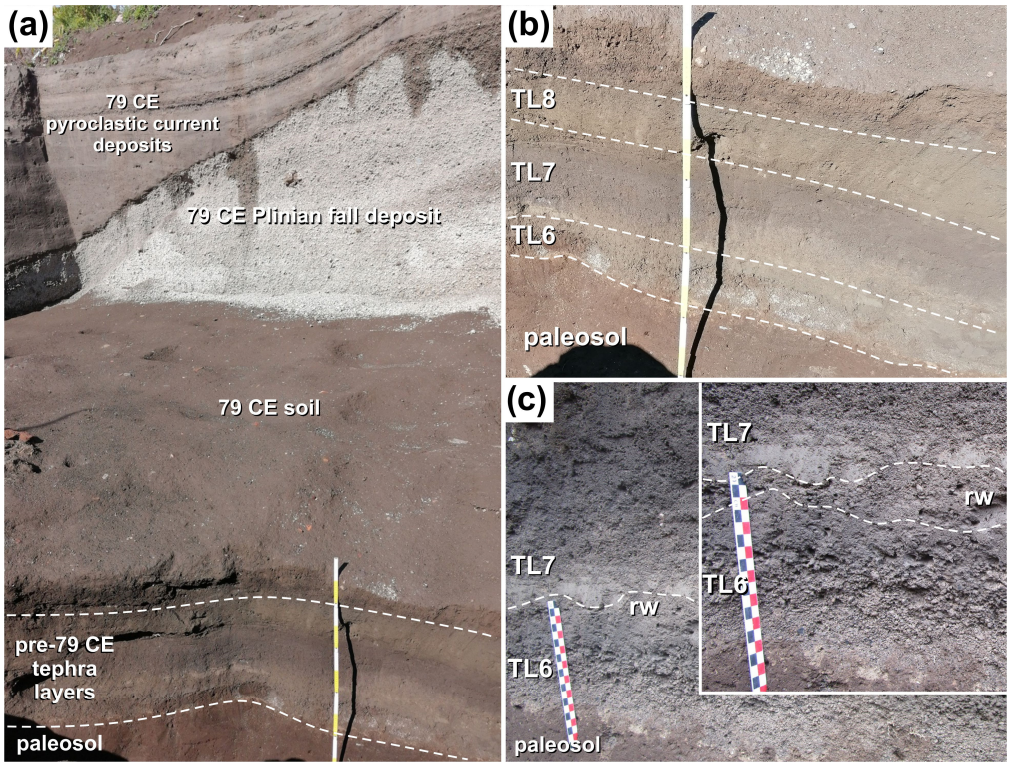

Figure 9. Trench VM (Villa dei Misteri): (**a**) sequence of tephra layers underlying the pyroclastic deposits of the 79 CE eruption; (**b**) close-up view of the pre-79 CE (protohistoric) tephra layers; (**c**) detail of TL6 (AP2 eruption) and TL7 (AP3 eruption) tephra. Note the undulated erosive surface on top of TL6 and the very limited thickness of reworked (rw) ash that separates TL6 and TL7 (between dashed lines).

TL7 has a total thickness of 44.5 cm, rests on reworked sediments on top of TL6 (Figures 8 and 9) and consists of two stratigraphic units (TL7-a and TL7-b; Figure 5g,h): TL7-a is a stratified deposit, 4.5 cm thick, consisting of two gray, massive, fine ash layers with sporadic accretionary lapilli separated by a very thin (≤0.5 cm) horizon of coarse ash. The thickness of the lower and upper ash layers is, respectively, 2.5–3 cm and 1.5 cm. TL7-b is a 40 cm thick, clast-supported, massive deposit consisting of angular, slightly porphyritic (pyroxene and biotite), fine lapilli to coarse ash. Juvenile clasts show various shades of gray ranging from predominant dark gray, dense to micro-vesiculated scoria to minor lighter-colored, moderately vesiculated pumice. Rare mm-sized lithic lava fragments are dispersed. The uppermost 20 cm is partly reworked, and the top is weakly humified. Two samples collected in trench CA6 (Figure 2), at the base (CA6/TL7b_base) and at the top (CA6/TL7b_top) of the scoria lapilli, show similar values (Table 2) of median diameter (0.72 and 0.75Φ) and sorting coefficient (1.19 and 1.16).

Finally, the uppermost TL8 is a very poorly preserved, massive, light gray, fine ash containing very fine pumice lapilli and accretionary lapilli. It has been recognized only in trenches CA6 and CA10 (Insula dei Casti Amanti, Figure 5g), VM (Figure 9) and S30 due to the extensive anthropic activity that has erased the upper part of the stratigraphic sequence.

The recognition in TL5 of a coarse pumice fragment emplaced as a projectile (clasts ejected during explosive eruptions moving along ballistic trajectories, e.g., [128,129]) gives clear and striking evidence of the proximity of the source (e.g., [130–132]), allowing a straightforward attribution of this tephra to Somma–Vesuvius. Furthermore, the occurrence of ballistic fragments more than 9 km from the source suggests that TL5 resulted from quite a large eruption. At first glance, a correlation to the ~3.9 ka Avellino Plinian eruption may be supposed on the basis of the stratigraphic position above the paleosol developed

on top of the Mercato tephra. However, this correlation is challenged when the chemical composition is taken into account. The sample from TL5 (Figure 6) possesses a composition that straddles the boundary between tephri-phonolite and latite (SiO_2 = 55.1 wt.%, alkali sum = 10.3 wt.%), falls just outside the Avellino eruption compositional field that ranges from phonolite to tephri-phonolite (e.g., [64,112]) and is consistent with the compositional field of the AP eruptions group [61]. Binary diagrams (Figure 7b) show a much more reliable correlation with the AP eruptions group as well. On the whole, AP eruptions show a slightly less evolved composition than the Avellino products, ranging from minor phonolite to mostly tephri-phonolite (Figure 6). Therefore, we rule out an attribution of TL5 to the Avellino eruption and suggest a much more confident correlation to the AP1 sub-Plinian eruption (3.7–3.5 ka [6,64,133]), whose juvenile material consists mainly of light-colored pumice [69]. The overlying TL6, TL7 and TL8 can be associated with Vesuvius activity as well (AP eruptions) based on the (1) chronostratigraphic position (3.5 ka bp–79 CE) and (2) tephri-phonolitic composition (TL6, SiO_2 = 54 wt.% and alkali sum = 10.1 wt.%; TL7, SiO_2 = 52.2 wt.% and alkali sum = 9.7 wt.%; TL8, SiO_2 = 52.6 wt.% and alkali sum = 10 wt.%) consistent with the compositional field of the AP eruptions group (Figures 6 and 7b). Indeed, following Epoch III of activity (5.5–3.5 ka, [78,79]), Campi Flegrei experienced a long-lasting period of quiescence, culminating in the Monte Nuovo eruption, which occurred in 1538 CE. Conversely, Ischia Island has been very active in the last 10 ky [84], with its products ranging from dominant trachyte to minor phonolite and latite, and rare shoshonite [134].

The stratigraphic framework, locally well-preserved, and the textural characteristics of TL6 and TL7 provide some important clues for a more specific attribution. Overall, both TL6 and TL7 are formed by a basal ash layer overlaid by a lapilli fall deposit. Such characteristics suggest a correlation with the AP2 sub-Plinian eruption (3.5–3.4 ka [64,133]) and AP3 Strombolian eruption (2.8–2.7 ka [64,135]), respectively. The AP2 sequence [69] consists of a basal fall deposit of light-colored pumice (bed A) followed by an accretionary lapilli-bearing ashfall deposit (bed B), and a lapilli deposit composed of gray pumice and dark-greenish scoria (bed C) in turn capped by a gray–greenish accretionary lapilli-bearing ashfall (bed D). TL6-a, TL6-b and TL6-c show characteristics that can be confidently correlated with beds A, C and D of AP2, respectively. This correlation is further supported by sedimentological data. Grain size data provided by Andronico and Cioni [69] indicate that bed C of the AP2 eruption is well-sorted and slightly reverse-graded as well as our stratigraphic unit TL6-b. The AP3 sequence [69] consists of a basal fine ash with minor coarse ash laminations (bed A) followed by a scoria fall deposit (bed B) and a sequence of faintly laminated, accretionary lapilli-bearing ash layers (bed C). The characteristics of TL7-a and TL7-b clearly correspond to beds A and B of AP3, respectively. Regarding TL8, due to its poor preservation, a more specific correlation is avoided. It may be associated with any of the remaining AP eruptions (AP4 to AP6), although a speculative correlation to the AP4 event (undated) is suggested.

7. Discussion

The recognition of several pre-79 CE tephra layers in Pompeii on top of the Pompeii bedrock permits some considerations on the chronostratigraphic and geoarchaeological evolution of the site, which is graphically summarized by the chronogram in Figure 10 and discussed below. Of the eight tephra layers clearly identified (plus a ninth, very poorly preserved, unidentified tephra), six were sourced from Somma–Vesuvius (Pomici Base, Mercato, plus four protohistoric "AP" eruptions) and two from Campi Flegrei (Neapolitan Yellow Tuff and Soccavo 4), spanning from the late Pleistocene to the Holocene (Upper Paleolithic to at least the Archaic archaeological period, Figure 10).

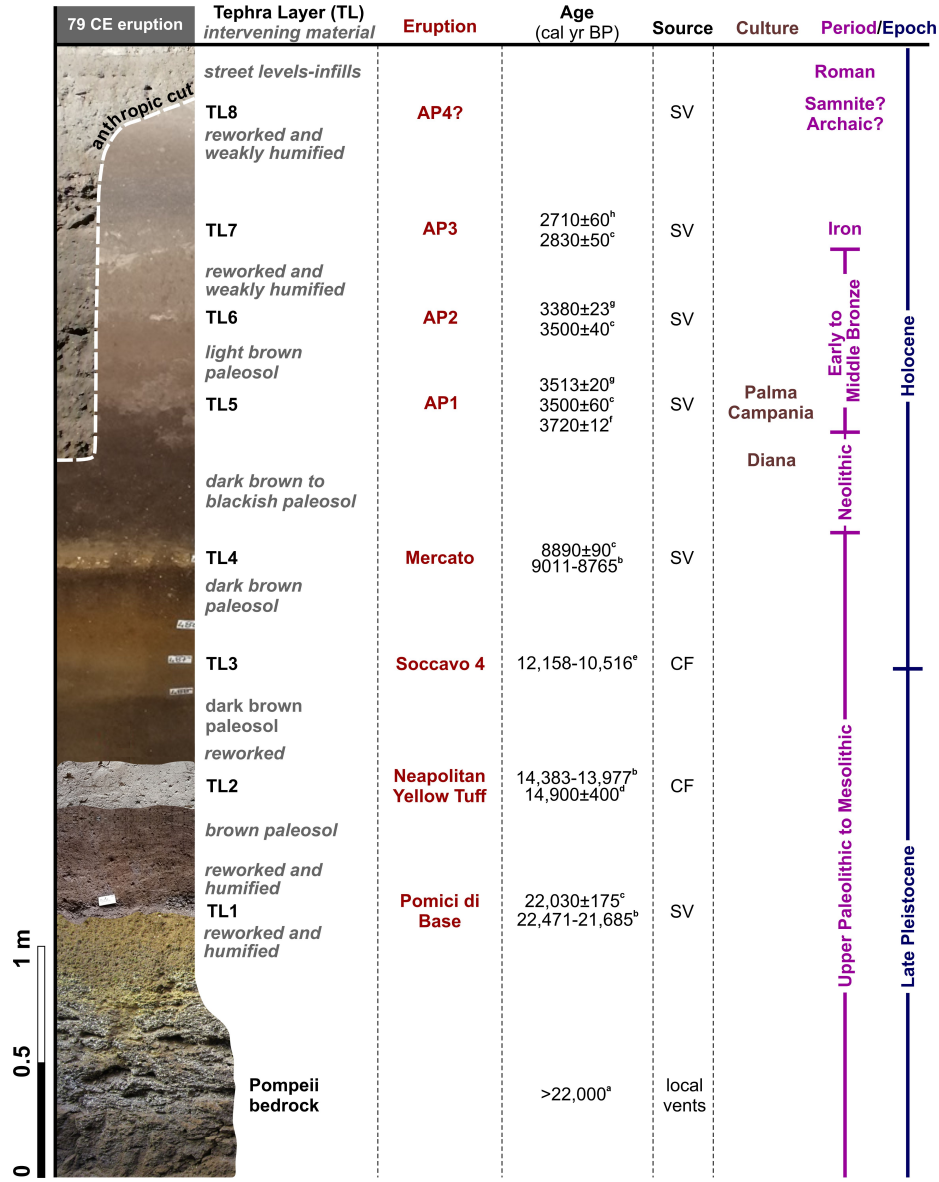

Figure 10. Chronogram showing the relationship among the pre-79 CE tephra layers (and intervening materials), eruption, age, source area, cultural facies, archaeological period and geological epoch at the Pompeii archaeological site. Source area: SV = Somma–Vesuvius; CF = Campi Flegrei. Age data sources: [a] this study, [b] [65], [c] [64], [d] [76], [e] [79], [f] [6], [g] [133], [h] [135]. The age of the Pompeii bedrock is constrained between 22 and 40 ka. Anthropic cuts (white dashed line) often truncate the Protohistoric unit (TL5 to TL8). In some cases, anthropic cuts can also affect the underlying units down to the Pompeii bedrock depending on the thickness of the terrains. Question mark (?) indicates uncertain attribution.

The uneven surface on the Pompeii bedrock, resulting in a basin-like morphology underlying the Insula dei Casti Amanti, favored the sedimentation and partial preservation of pyroclastic deposits, followed by the aggradation of reworked volcaniclastic materials, which underwent pedogenetic processes. Prehistoric (Upper Paleolithic to Neolithic, Figure 10) tephra layers suffered extensive reworking processes and are often poorly preserved, whilst protohistoric (Bronze Age to Archaic period) "AP" tephra layers are often wiped out by anthropic cuts and infills. Although a paleoenvironmental reconstruction is out of the scope of this paper, it is worth noting that no evidence of shallow marine environmental conditions (tephra emplaced in shallow waters or shallow marine sediments) was found throughout the stratigraphic succession, suggesting the persistence of sub-aerial

conditions in this area. As already clearly stressed by Amato et al. [44], the uplift proposed by Marturano et al. [42,45] appears inconsistent with the lithostratigraphic characteristics of the studied succession. In these sub-aerial environmental conditions, stages characterized by volcanic quiescence, and without continuous aggradation of reworked volcaniclastic deposits, resulted in the formation of well to poorly developed paleosols.

7.1. Chronostratigraphic Evolution of the Pompeii Site

7.1.1. Late Pleistocene

The chronostratigraphic evolution of the Pompeii site began at ~40 ka bp, when the Campanian Ignimbrite eruption (Campi Flegrei) occurred. This large explosive event (magnitude M between 7.2 and 7.7 [97,99]) buried the Sarno plain, as well as most of the Campania region, under a thick ignimbrite sheet (e.g., [96–100]). This catastrophic eruption took place in a period of cultural changes, which included the Middle to Upper Paleolithic transition in Europe (e.g., [102,136,137]). After the Campanian Ignimbrite eruption, volcanic activity occurred in the Pompeii area through local vents from which lavas and pyroclastic products (scoriaceous to spatter fragments) had erupted. Lavas and pyroclastic products accumulated close to the vents forming the geological framework (Pompeii bedrock) of the small volcanic relief on which Pompeii was built. The macroscopic characteristics of the spatter deposits cropping out in the Insula Meridionalis (Figure 3), such as coarseness and the welding degree, are consistent with a very proximal deposition. A possible location of the vent area is in the western to northwestern part of the archaeological site, as inferred from the S-SE dipping of the welded spatter layers. This is also consistent with the presence of multiple coalesced crater rims in the western part of Pompeii [31]. The association of lavas and scoriaceous to spatter deposits suggests the occurrence of both effusive and low-energy explosive activity from these vents. Welded spatter horizons resulted from Hawaiian-style lava-fountaining episodes, which usually last from hours to days (e.g., [138–140]) and were emplaced as fall deposits. Deposition from spatter-rich pyroclastic currents can be ruled out owing to the lack of an ash matrix, clast imbrication, association with matrix-supported deposits, normal or reverse-graded structure, topographically controlled deposition and lateral or vertical transition into lithic breccias (e.g., [140–147]). Spatter deposits of the Pompeii bedrock show a range of welding degrees, from highly welded to poorly welded/unwelded lithofacies. Welded lithofacies, associated with flattened clast morphologies with high aspect ratios, indicate that fragments were fluidal, sticky and hot enough to deform and weld upon landing and after deposition. Since the aspect ratio of the individual large fragments appears to be constant upward, the flattening is attributed to the kinetic impact upon landing rather than load compaction. The process of welding of spatter fragments results mainly from a combination of different parameters: the accumulation rate, the temperature of deposition and the deposit heat loss (e.g., [109,110,138,139,148–151]). The ejection of incandescent magma clots, with minimal in-flight cooling, emplaced at high accumulation rates caused the resultant deposit to coalesce or weld along the contact points between the fragments. The rapid aggradation of the deposit, up to several meters, prevented efficient heat loss, which, in turn, further promoted the agglutination/welding process. The general upward decrease in the welding degree, from apparently coherent spatter to dense spatter lithofacies, records a progressively lower accumulation rate, which enhanced the deposit heat loss and prevented complete welding. The uppermost poorly welded to unwelded (vuggy spatter) lithofacies resulted from the lowest accumulation rate and emplacement temperature. Coarse scoriaceous deposits strictly associated with spatter deposits suggest the occurrence of weak Strombolian phases during the same eruption(s) [110].

New insights into the upper chronological constraint of the Pompeii bedrock arise from the investigation of the stratigraphic succession on top of it. The lowermost and oldest tephra (TL1) is associated with the 22 ka Pomici di Base Plinian eruption. The products of this eruption crop out in natural exposures and quarries on the northern Mt. Somma slope. Conversely, they are buried under a thick succession of younger deposits on the sea side (south) of the volcano [113] and have been clearly recognized in boreholes along a transect to the southwest [94] of Vesuvius. The clear recognition of the Pomici di Base tephra in Pompeii is in agreement with the finding reported by Rolandi et al. [93] from an excavation near Porta Nocera. This allows us to definitively attribute a relative age older than 22 ka to the Pompeii bedrock (40–22 ka), as already previously suggested by Rolandi et al. [93] and Di Vito et al. [94]. In the same time span (40–22 ka), the ancient edifice (current Mt. Somma) grew through the superimposition of lavas and pyroclastic deposits [61,63]. The presence of a poorly developed, reddish, reworked and weakly humified volcaniclastic layer, containing leucite-bearing lava fragments, between TL1 and the underlying lava indicates that the Pomici di Base eruption may shortly postdate the emplacement of this (uppermost) lava of the Pompeii bedrock, though a marked erosional phase cannot be excluded. The Pompeii bedrock is also coeval with several ancient (>22 ka) lateral vents on the Mt. Somma flanks, whose activity resulted in the formation of small scoria- and spatter-cones [110]. Such cones are mantled by the Pomici di Base pyroclastic products with a thin paleosol in between [110,152]. An $^{40}Ar/^{39}Ar$ age of 23.6±0.3 ka has been obtained for one of these ancient cones (Traianello cone [110]) suggesting that such cone-forming eruptions are chronologically close to the upper limit of the pre-caldera period (40–22 ka) of Somma–Vesuvius. The local volcanic activity in the Pompeii area possibly occurred in the same timeframe based on the field evidence.

Following the Pomici di Base eruption, a marked phase of erosion and reworking resulted in a decimeter-thick, reworked, volcaniclastic deposit, whose upper part underwent pedogenetic processes. This phase likely lasted until the sedimentation of TL2 associated with the 15 ka NYT eruption of Campi Flegrei. No traces of other tephra layers have been detected between the Pomici di Base and NYT. The occurrence of the NYT at Pompeii is consistent with the finding of this tephra in cores as far as the Poseidonia-Paestum archaeological area (~56 km southeast of Pompeii [153]) and the San Gregorio Magno basin (~80 km east of Pompeii [154]). In addition, Rittmann [101], as also mentioned by Ippolito [155], reported the finding at Pompeii (well dug in the Casa dei Vasi di Vetro; Vas in Figure 2) of a pyroclastic deposit they attributed to the NYT eruption. Following the NYT eruption, a new phase of erosion, reworking and pedogenesis occurred. This phase culminated in the formation of a brown paleosols, 40 cm thick, capped by another tephra layer (TL3) from Campi Flegrei, associated with the 10.5–12.1 ka Soccavo 4 eruption, in turn grading in a well-developed dark brown paleosol. The paleosol underlying TL3 shows, in its upper half, haloes of a very poorly preserved and humified, grayish ash, representing the contribution of an unidentified eruptive event. This ash likely did not completely bury the soil and, consequently, did not cut it off from a continuous soil formation process, resulting in rapid incorporation and pedogenesis of the fresh volcanic material [41]. In the period between the NYT and Soccavo 4 eruptions, the Campi Flegrei caldera was very active [78,79]; thus, it represents the most reliable volcanic source for these ash traces (possibly the 11.9–12.1 ka Pomici Principali eruption). In addition, traces of prehistoric (Late Pleistocene), very weathered ash layers have been also found in other archaeological trenches dug at Pompeii [49]. The sedimentation of TL3 occurred around the late Pleistocene–Holocene transition (Figure 10), which indicatively corresponds to the Upper Paleolithic–Mesolithic transition [156] in Europe.

7.1.2. Holocene

At 8.9 ka bp, the second caldera-forming eruption of Somma–Vesuvius occurred (Mercato eruption), the deposits of which at Pompeii consist of white pumice fragments in a yellow–orange ash matrix. Due to its easily recognizable characteristics and almost ubiquitous presence (it has been recognized in trenches in different parts of Pompeii, e.g., [29,106,157–159]), we consider this tephra layer a chronostratigraphic marker in the pre-79 CE succession at Pompeii. The pyroclastic products of the Mercato eruption represent the parent material of a thick, dark and very mature paleosol. This paleosol reflects a long period (~5000 years) of volcanic quiescence falling within the Holocene climatic optimum, which promoted soil development (e.g., [160]). These beneficial conditions favored the earliest human occupation of the Pompeii area in the late Neolithic [29,45]. The formation of this paleosol spans the Mesolithic–Neolithic transition, which in Southern Italy is dated between seventh and sixth millennia BCE [161]. In detail, the process of Neolithization of southern Italy occurred between 6200 and 5700 BCE and is represented by Archaic Impressed Ware cultural horizons [162], whilst the first human occupation of the Pompei area is represented by material fragments of the Diana culture [29] (Figure 10), diffused between 4300 and 3700 BCE [30]. This means that the early occupation of the Pompeii area occurred ~2000 years after the Mesolithic–Neolithic transition.

This ~5 ky long period of volcanic quiescence culminated in the 3.9 ka Avellino Plinian eruption. No traces of this eruption have been found in the investigated trenches, and its possible impact on the Pompeii area is discussed in the following section. Then, four protohistoric eruptions of Somma–Vesuvius affected Pompeii (Figure 10): two sub-Plinian events (AP1 and AP2) between ~3.7 and ~3.4 ka bp, a violent strombolian eruption (AP3) at 2.8–2.7 ka bp and a fourth later undated event (AP4). Our attributions do not match the results of Robinson [50], which point to the occurrence, in the same chronostratigraphic interval, of four tephra layers attributed to the activity of Campi Flegrei (likely two Astroni eruptions), Somma–Vesuvius (an AP eruption) and Ischia (Cannavale tephra). A direct comparison is impractical as the author bases his chronostratigraphic interpretation on the radiocarbon ages of organic findings and the statistical analysis of the available (at the time) ages of the eruptions of the Neapolitan volcanoes. Conversely, our results appear consistent with the stratigraphy proposed by Ranieri [48], which indicated the presence at Pompei of at least three AP events.

The stratigraphy of the Protohistoric unit raises some concerns about the consistency of the available age determinations with respect to the field characteristics. Such consistency has already been questioned in the past (e.g., [41,64]). The age of the AP (Protohistoric) eruptions appears to be inconsistent with the observed characteristics of the intervening deposits at Pompeii. Most age determinations [64,133,163] suggest a time span no longer than a few decades between the AP1 and AP2 events, which, according to the cited authors, occurred ~3.5 ka bp (Figure 10). The occurrence of a distinct soil, 30 cm thick, between TL5 and TL6 (AP1 and AP2) suggests a longer break in the volcanic activity, as a short time interval (few decades) would not result in a well-defined soil [41]. A thin paleosol between AP1 and AP2 deposits is also reported by Andronico and Cioni [69]. The AP2 eruption was followed, based on the available age determinations, by 500–700 years of quiescence culminating in the 2.8–2.7 ka AP3 eruption (Figure 10). Also, in this case, the presence between TL6 and TL7 (AP2 and AP3) of a reworked deposit, locally just a few centimeters thick (VM trench, Figure 9), showing at most very weakly developed pedogenetic transformations, is in contrast with such a long rest (Andronico and Cioni [69] reported just a discontinuous, thin, humified layer underlying the AP3 sequence). Similarly, Vogel et al. [41] describe only initial pedogenetic transformations of ash layers attributed to AP2 and AP3 eruptions in an excavation near Scafati (~3 km E-NE of Pompeii). The pre-79 CE sequence is closed by a

poorly preserved ash layer (TL8), tentatively attributed to the AP4 eruption, resting on the reworked and slightly humified top of TL7, suggesting a short period of rest.

7.2. Geoarchaeological Implications: Insights into the Avellino Eruption in the Pompeii Area

Evidence of the human presence in the eastern Campanian Plain dates back to the Upper Paleolithic and Mesolithic [164]. The first evidence of human occupation in the Pompeii area dates back to the late Neolithic [29]. The following level of occupation dates back to the EBA. Compared to other areas around Vesuvius or in the Campanian Plain [164], the Pompeii site does not show evidence of a continuous human presence from the late Neolithic to the EBA to Iron Age (e.g., [165]). The evidence of the human presence during the EBA comes from pottery fragments of the Palma Campania culture found in association with a tephra layer speculatively attributed to the 3.9 ka Avellino eruption [27,28]. The association between the Avellino eruption and the EBA in the Campania region is well-established in the areas directly affected by the eruption due to the high number of available radiocarbon ages (e.g., [66]). The composite Avellino pyroclastic sequence consists of a white to gray Plinian fall deposit, dispersed over a wide area to the northeast of Somma–Vesuvius (e.g., [121]), and pyroclastic current deposits sealing a large area mostly to the north and northwest of the volcano (e.g., [166]). The eruption had a significant impact, affecting many EBA villages as well as the landscape around Vesuvius (e.g., [5,6,167–172]), with only sporadic resettlements of the sites abandoned prior to or during the eruption. This may be due to the frequent post-eruption remobilization of pyroclastic products with emplacement of volcaniclastic mass flow deposits [6]. However, in Pompeii and nearby areas, the occurrence of the Avellino tephra in the geoarchaeological stratigraphy has been speculated. The straightforward attribution of tephra layers found in association with the EBA Palma Campania cultural layers to the Avellino eruption (e.g., [27,28]) has been challenged for many years (e.g., [6,172,173]). On the other hand, in an excavation in Scafati (3 km E-NE of Pompeii), Vogel et al. [41] recognized, for the first time in the area, faint traces of the Avellino tephra overlying a paleosol bearing EBA pottery fragments. The Pompei area was possibly only marginally affected by the Avellino eruption, and only few traces may be related to the eruption according to Albore Livadie et al. [172]. In Pompeii, the tephra layer associated with the Avellino eruption has been described as a hardened, light gray ash containing fine lapilli [27,28]. A similar tephra has also been reported in the nearby S. Abbondio site [174], <1 km to the southeast of Pompeii (Figure 1), whose early occupation dates to the late Neolithic (Diana culture) and Eneolithic (Laterza culture) [175]. The S. Abbondio site is located at the southern end of the Pompeii bedrock (Figure 1), overlooking the surrounding plain. Controversial interpretations exist about the attribution of tephra layers found in the geoarchaeological stratigraphy of this site [165,174–177]. The reorganization of the field data from past excavations, edited in recent years by one of the authors (P. Talamo), promoted a more confident interpretation of the geoarchaeological stratigraphy of the S. Abbondio site, which along with our chronostratigraphic data within Pompeii, can provide insights into the occurrence of the Avellino eruption in the Pompeii area. The intended use of the S. Abbondio site changed through time, from a settlement of the EBA Palma Campania culture to a burial site belonging to a transitional phase from the EBA Palma Campania to the Middle Bronze Age Proto-Apennine culture [175]. The occupation level of the EBA Palma Campania settlement is represented by a reddish to brownish volcaniclastic layer arising from the weathering of the underlying Pompeii bedrock. Pole holes cut through this layer down to the Pompeii bedrock. The paleosurface of the Palma Campania settlement is covered by a yellowish sandy layer that bears traces of a thin, mainly reworked tephra layer (hereafter, the first ash layer) toward the base. This tephra, which marks the first abandonment of the site (settlement), has been associated

with the Avellino eruption based on its stratigraphic position [175]. The site was later re-occupied, although its function was significantly modified, becoming a burial site, which was in use for less than two centuries, with a transition of the cultural phase from Palma Campania to the Proto-Apennine 1 or 2 (Early to Middle Bronze Age), until the definitive protohistoric abandonment (e.g., [6]). The burials are cut through the yellowish sandy layer, the surface of which represents the occupation level of the burial site. The graves are buried by a grayish "alluvial–colluvial" deposit containing another ash layer (hereafter, the second ash layer) resulting from an eruption younger than the Avellino event (an AP eruption). This view is also supported by an early interpretation [165], which suggested that the S. Abbondio burial site was affected by "Eruption A" of Albore Livadie et al. [178], tentatively dated to the XI-X century BCE based on archaeological constraints, which corresponds to an AP event. A different view is provided by Calderoni and Russo [176] and Pappalardo et al. [177], who attribute the tephra layer that seals the burial site, described as a ~15 cm thick gray ash horizon, to the Avellino eruption based on the radiocarbon age (2110–2100 years BCE [170]) of a charcoal fragment, likely a hearth relic, coming from an erosional task cut into the soil underlying the ash layer.

Our stratigraphic and geochemical characterization has highlighted that a well-defined layer, or even faint traces, associated with the Avellino eruption is lacking in all twenty-one trenches investigated in various sectors of ancient Pompeii. Nonetheless, we cannot completely exclude, based on the literature data as well as the reappraisal of the S. Abbondio geoarchaeological stratigraphy, the possibility that the Avellino eruption affected, albeit minimally, the Pompeii area, emplacing a very thin and very poorly preserved tephra (first ash layer in the S. Abbondio stratigraphy), later rapidly wiped out by reworking, pedogenesis and anthropic activity. According to Di Vito et al. [6], the proximity to the volcano and the catastrophic phenomena that occurred during the Avellino eruption probably led the inhabitants to temporarily abandon the area. We also suggest that, as already speculated by previous authors [6,172,173], the well-defined ash horizon found in association with the Palma Campania cultural layers within Pompeii and sealing the S. Abbondio burials (second ash layer) resulted from an eruption younger than the Avellino Plinian event, which, based on our composite stratigraphy, is identified in the 3.7–3.5 ka AP1 eruption (our TL5 unit), classified as a sub-Plinian type II event [179]. Sub-Plinian type II eruptions are characterized by oscillating eruptive columns and ash emissions lasting from days to weeks, whose impact on the territory and communities may be relevant due to the duration, although they represent the less energetic end member in the spectrum of Plinian/sub-Plinian activity [179]. Our attribution validates the stratigraphic interpretation provided in [175], which suggests that the transformation from inhabited area to burial site at S. Abbondio postdates the Avellino eruption. Lasty, our results are supported by the absence of the Avellino deposits in cores drilled just south of the Pompeii archaeological site [32,44,94].

8. Conclusions

Humans and volcanoes have a long history of cohabitation in the Campania region, which conditioned human societies, activities and, possibly, migrations (e.g., [11,12,164]). The ancient city of Pompeii is part of this history. As for the 79 CE eruption and its devastating effects on the city, the contribution of volcanology can be extremely useful and complementary to archaeology for the investigation of pre-Roman layers in Pompeii. Indeed, the clear recognition and attribution of tephra layers to well-known and dated eruptions add value to the archaeological investigation, providing a more precise chronostratigraphic constraint on archaeological finds. As a matter of fact, tephra layers are isochronous surfaces emplaced during a geologically instantaneous event (explosive

eruption), whose age (if known) can be also useful for a relative dating of archaeologically barren materials. Our results, based on the stratigraphic survey of twenty-one trenches throughout Pompeii, provide evidence of a composite, pre-79 CE stratigraphy consisting of at least eight tephra layers, representing ~20,000 years of volcanic history (late Pleistocene to Holocene), interlayered with buried soils, volcanoclastic reworked deposits, and human occupation dating back to the late Neolithic and EBA. Tephra layers resulted from explosive activity associated with a range of eruption types, from Plinian/sub-Plinian to Strombolian events, from Vesuvius (Pomici di Base, Mercato and AP1 to AP4) and Campi Flegrei (Neapolitan Yellow Tuff and Soccavo 4). The volcanic rocks (lavas and scoriaceous to spatter deposits) of the Pompeii bedrock, which constitute the geological framework of the small relief on which ancient Pompeii was built, are the result of effusive activity and Hawaiian-style lava-fountaining to weak Strombolian phases from local vents. The last activity of these local vents occurred not long before the 22 ka Pomici di Base eruption, the deposits of which have been clearly detected on top of the Pompeii bedrock via interposition of thin reworked volcaniclastic materials. This activity is coeval with many scoria- and spatter-cones on the Mt. Somma flanks, older than the Pomici di Base eruption [110].

Lastly, we recommend taking caution in the attribution of Bronze Age tephra layers to specific eruptions during future archaeological investigations in Pompeii, as our outcomes point to the occurrence of two well-defined Middle Bronze Age tephra (AP1 and AP2 eruptions). No traces (even faint) of a tephra associated with the 3.9 ka Avellino eruption (Early Bronze Age) were detected in any trenches, although data from the nearby S. Abbondio site suggest that this Plinian eruption could have marginally affected the Pompeii area, resulting in a very thin ash layer wiped out by erosion/reworking and, possibly, locally preserved as small lenses.

Author Contributions: D.S. performed the stratigraphic survey of 20 out of 21 trenches, sampling and sedimentological analyses, analyzed the data, conceived the paper and wrote the first and revised manuscripts. V.A. (Vincenzo Amato) and M.A.D.V. contributed to the stratigraphic survey and sampling. A.R. provided stratigraphic data and photos of trench S16. P.T. edited the reappraisal of the stratigraphic data of the S. Abbondio site. V.A. (Valeria Amoretti) and G.Z. secured the archaeological setting. All authors have read and agreed to the published version of the manuscript.

Funding: This research received no external funding.

Data Availability Statement: The original contributions presented in this study are included in the article, and further inquiries can be directed to the corresponding author.

Acknowledgments: We are grateful to Daniele Alessi, Luca Borsa, Pasqualina Buondonno, Andrea Chiatroni, Tommaso Conti, Dora D'Auria, Angelo Mazzocchi, Gloria Ortino, Viviana Petraroli, Luca Salvatori, Maria Vallifuoco and Teresa Virtuoso for their archaeological assistance during fieldwork. We are indebted to Vincenzo Calvanese, Alberta Martellone, Raffaele Martinelli, Crescenzo Mazzuoccolo, Paolo Mighetto, Antonino Russo and Giuseppe Scarpati, officers of the Parco Archeologico di Pompei, for their helpfulness in granting us access to all sites. We extend our gratitude to Massimo Osanna, former Director of the Parco Archeologico di Pompei. Marina Loddo is acknowledged for her help with the literature search. Heartfelt thanks go to Carlo Pelullo for his "geochemical" support. Comments and suggestions provided by three anonymous reviewers have been greatly appreciated and contributed to improving the manuscript.

Conflicts of Interest: The authors declare no conflicts of interest.

References

1. Cashman, K.V.; Giordano, G. Volcanoes and human history. *J. Volcanol. Geotherm. Res.* **2008**, *176*, 325–329. [CrossRef]
2. Sheets, P. Volcanoes, ancient people, and their societies. In *The Encyclopedia of Volcanoes*; Sigurdsson, H., Ed.; Academic Press: London, UK, 2015; pp. 1313–1319.

3. Sheets, P. Volcanoes and People. In *Encyclopedia of Geoarchaeology. Encyclopedia of Earth Sciences Series*; Gilbert, A.S., Ed.; Springer: Dordrecht, The Netherlands, 2017; pp. 1001–1006. [CrossRef]
4. Di Vito, M.A.; Sparice, D.; de Vita, S.; Doronzo, D.M.; Ricciardi, G.P.; Uzzo, T. The Museum of the Osservatorio Vesuviano: Inviting the public to explore the geoheritage of the world's first volcano observatory. *Bull. Volcanol.* **2023**, *85*, 45. [CrossRef]
5. Di Vito, M.A.; Zanella, E.; Gurioli, L.; Lanza, R.; Sulpizio, R.; Bishop, J.; Tema, E.; Boenzi, G.; Laforgia, E. The Afragola settlement near Vesuvius, Italy: The destruction and abandonment of a Bronze Age village revealed by archaeology, volcanology and rock-magnetism. *Earth Planet. Sci. Lett.* **2009**, *277*, 408–421. [CrossRef]
6. Di Vito, M.A.; Talamo, P.; de Vita, S.; Rucco, I.; Zanchetta, G.; Cesarano, M. Dynamics and effects of the Vesuvius Pomici di Avellino Plinian eruption and related phenomena on the Bronze Age landscape of Campania region (Southern Italy). *Quat. Int.* **2019**, *499*, 231–244. [CrossRef]
7. Scarpati, C.; Perrotta, A.; De Simone, G.F. Impact of explosive volcanic eruptions around Vesuvius: A story of resilience in Roman time. *Bull. Volcanol.* **2016**, *78*, 21. [CrossRef]
8. Amato, V. Geoarchaeology: A Review of Case Studies in the Mediterranean Sea. *Geosciences* **2021**, *11*, 42. [CrossRef]
9. de Vita, S.; Di Vito, M.A.; Gialanella, C.; Sansivero, F. The impact of the Ischia Porto Tephra eruption (Italy) on the Greek colony of Pithekoussai. *Quat. Int.* **2013**, *303*, 142–152. [CrossRef]
10. de Vita, S.; Di Vito, M.A.; Barra, D.; Aiello, G.; Gialanella, C. Disseminating the knowledge on the complex interactions between humans and volcanoes: The geological section of the Villa Arbusto archaeological museum at Lacco Ameno (Ischia, Naples-Italy). *Ann. Geophys.* **2021**, *64*, VO544. [CrossRef]
11. Di Vito, M.A.; Aurino, P.; Boenzi, G.; Laforgia, E.; Rucco, I. Human communities living in the Central Campania plane and eruptions of Vesuvio and Campi Flegrei since Neolithic. *Ann. Geophys.* **2021**, *64*, VO546. [CrossRef]
12. Costa, A.; Di Vito, M.A.; Ricciardi, G.P.; Smith, V.C.; Talamo, P. The long and intertwined record of humans and the Campi Flegrei volcano (Italy). *Bull. Volcanol.* **2022**, *84*, 5. [CrossRef]
13. Sigurdsson, H.; Carey, S.; Cornell, W.; Pescatore, T. The eruption of Vesuvius in A.D. 79. *Natl. Geogr. Res.* **1985**, *3*, 332–397.
14. Cioni, R.; Gurioli, L.; Sbrana, A.; Vougioukalakis, G. Precursory phenomena and destructive events related to the Late Bronze Age Minoan (Thera, Greece) and AD 79 (Vesuvius, Italy) Plinian eruptions; inferences from the stratigraphy in the archaeological areas. *Geol. Soc. Lond. Spec. Publ.* **2000**, *171*, 123–141. [CrossRef]
15. Luongo, G.; Perrotta, A.; Scarpati, C. Impact of the AD 79 explosive eruption on Pompeii, I. Relations amongst the depositional mechanisms of the pyroclastic products, the framework of the buildings and the associated destructive events. *J. Volcanol. Geoth. Res.* **2003**, *126*, 201–223. [CrossRef]
16. Luongo, G.; Perrotta, A.; Scarpati, C.; De Carolis, E.; Patricelli, G.; Ciarallo, A. Impact of the AD 79 explosive eruption on Pompeii, II. Causes of death of the inhabitants inferred by stratigraphic analysis and areal distribution of the human casualties. *J. Volcanol. Geoth. Res.* **2003**, *126*, 169–200. [CrossRef]
17. Gurioli, L.; Pareschi, M.T.; Zanella, E.; Lanza, R.; Deluca, E.; Bisson, M. Interaction of pyroclastic density currents with human settlements: Evidence from ancient Pompeii. *Geology* **2005**, *33*, 441. [CrossRef]
18. Scandone, R.; Giacomelli, L.; Rosi, M. Death, survival and damage during the 79 AD eruption of Vesuvius which destroyed Pompeii and Herculaneum. *J. Res. Didact. Geogr.* **2019**, *2*, 5–30.
19. Scarpati, C.; Perrotta, A.; Martellone, A.; Osanna, M. Pompeian hiatuses: New stratigraphic data highlight pauses in the course of the AD 79 eruption at Pompeii. *Geol. Mag.* **2020**, *157*, 695–700. [CrossRef]
20. Doronzo, D.M.; Di Vito, M.A.; Arienzo, I.; Bini, M.; Calusi, B.; Cerminara, M.; Corradini, S.; de Vita, S.; Giaccio, B.; Gurioli, L.; et al. The 79 CE eruption of Vesuvius: A lesson from the past and the need of a multidisciplinary approach for developments in volcanology. *Earth Sci. Rev.* **2022**, *231*, 104072. [CrossRef]
21. Scarpati, C.; Chiominto, G.; Santangelo, I.; Perrotta, A.; Fedele, L. The 79 AD Vesuvius eruption revisited: Plinian and post-Plinian falls. *J. Geol. Soc.* **2024**, *182*, jgs2024-071. [CrossRef]
22. Scarpati, C.; Santangelo, I.; Chiominto, G.; Perrotta, A.; Branney, M.J.; Fedele, L. The 79 AD Vesuvius eruption revisited: The pyroclastic density currents. *J. Geol. Soc.* **2024**, *182*, jgs2024-072. [CrossRef]
23. Sparice, D.; Amoretti, V.; Galadini, F.; Di Vito, M.A.; Terracciano, A.; Scarpati, G.; Zuchtriegel, G. A novel view of the destruction of Pompeii during the 79 CE eruption of Vesuvius (Italy): Syn-eruptive earthquakes as an additional cause of building collapse and deaths. *Front. Earth Sci.* **2024**, *12*, 1386960. [CrossRef]
24. Pilli, E.; Vai, S.; Moses, V.C.; Morelli, S.; Lari, M.; Modi, A.; Diroma, M.A.; Amoretti, V.; Zuchtriegel, G.; Osanna, M.; et al. Ancient DNA challenges prevailing interpretations of the Pompeii plaster casts. *Curr. Biol.* **2024**, *34*, 5307–5318. [CrossRef] [PubMed]
25. Varone, A. *Pompei, i Misteri di Una Città Sepolta: Storia e Segreti di un Luogo in Cui la Vita si è Fermata Duemila Anni fa*; Newton and Compton: Rome, Italy, 2000; pp. 1–364.
26. Geertman, H. The urban development of the pre-Roman city. In *The World of Pompeii*; Dobbins, J.J., Foss, P.W., Eds.; Routledge: New York, NY, USA; London, UK, 2007; pp. 124–139.

27. Nilsson, M. Evidence of Palma Campania settlement at Pompeii. In *Nuove Ricerche Archeologiche Nell'area Vesuviana (Scavi 2003–2006), Atti del Convegno Internazionale, Roma, Italy, 1–3 February 2007*; Studi della Soprintendenza archeologica di Pompei; L'Erma" di Bretschneider: Roma, Italy, 2008; Volume 25, pp. 81–86.
28. Boman, H.; Nilsson, M. The early street and the prehistoric finds in Vicolo delle Nozze d'Argento, Pompeii. *Opusc. Romana* **2008**, *31*, 161–165.
29. Varone, A. Per la storia recente, antica e antichissima del sito di Pompei. In *Nuove Ricerche Sull'area Vesuviana (Scavi 2003–2006), Proceedings of the Atti del Convegno Internazionale, Roma, Italy, 1–3 February 2007*; Studi della Soprintendenza Archeologica di Pompei; L'Erma" di Bretschneider: Roma, Italy, 2008; Volume 25, pp. 349–362.
30. Malone, C. The Italian Neolithic: A synthesis of research. *J. World Prehist.* **2003**, *17*, 235–312. [CrossRef]
31. Amato, V.; Covolan, M.; Dessales, H.; Santoriello, A. Seismic Microzonation of the Pompeii Archaeological Park (Southern Italy): Local Seismic Amplification Factors. *Geosciences* **2022**, *12*, 275. [CrossRef]
32. Aiello, G.; Amato, V.; Amoretti, V.; Barra, D.; Di Vito, M.A.; Doronzo, D.M.; Infante, A.; Russo, A.; Sparice, D.; Zuchtriegel, G. Marine Environments in Front of the Ancient City of Pompeii (Southern Italy) at 79 CE: New Insights for the Unknown Location of the Harbour. *Land* **2024**, *13*, 1198. [CrossRef]
33. Cinque, A.; Russo, F. La linea di costa del 79 d.C. fra Oplonti e Stabiae nel quadro dell'evoluzione olocenica della Piana di Sarno (Campania). *Boll. Soc. Geol. It.* **1986**, *105*, 111–121.
34. Barra, D.; Bonaduce, L.; Brancaccio, L.; Cinque, A.; Ortolani, F.; Pagliuca, S.; Russo, F. Evoluzione olocenica della piana costiera del Fiume Sarno (Campania). *Mem. Soc. Geol. Ital.* **1989**, *42*, 255–267.
35. Albore Livadie, C.; Barra, D.; Bonaduce, G.; Brancaccio, L.; Cinque, A.; Ortolani, F.; Pagliuca, S.; Russo, F. Evoluzione geomorfologica, neotettonica e vulcanica della piana costiera del fiume Sarno (Campania) in relazione agli insediamenti anteriori all'eruzione del 79 d.C. *Pact* **1990**, *25*, 237–256.
36. Pescatore, T.; Senatore, M.R.; Capretto, G.; Lerro, G. Holocene coastal environments near Pompeii before the AD 79 eruption of Mount Vesuvius, Italy. *Quat. Res.* **2001**, *55*, 77–85. [CrossRef]
37. Pescatore, T.; Senatore, M.R.; Capretto, G.; Lerro, G.; Patricelli, G. Ricostruzione paleo ambientale delle aree circostanti l'antica città di Pompei (Campania, Italia, al tempo dell'eruzione del Vesuvio del 79 d.C. *Boll. Soc. Geol. Ital.* **1999**, *118*, 243–254.
38. Di Maio, G.; Stefani, G. Considerazioni sulla linea di costa del 79 d.C. e sul porto dell'antica Pompei. *Riv. Studi Pompeiani* **2004**, *14*, 141–195.
39. Vogel, S.; Märker, M. Reconstructing the Roman topography and environmental features of the Sarno River Plain (Italy) before the AD 79 eruption of Somma–Vesuvius. *Geomorphology* **2010**, *115*, 67–77. [CrossRef]
40. Vogel, S.; Märker, M.; Seiler, F. Revised modelling of the post-AD 79 volcanic deposits of Somma-Vesuvius to reconstruct the pre-AD 79 topography of the Sarno River plain (Italy). *Geol. Carpathica* **2011**, *62*, 5. [CrossRef]
41. Vogel, S.; Märker, M.; Rellini, I.; Hoelzmann, P.; Wulf, S.; Robinson, M.; Steinhübel, L.; Di Maio, G.; Imperatore, C.; Kastenmeier, P.; et al. From a stratigraphic sequence to a landscape evolution model: Late Pleistocene and Holocene volcanism, soil formation and land use in the shade of Mount Vesuvius (Italy). *Quat. Int.* **2016**, *394*, 155–179. [CrossRef]
42. Marturano, A.; Aiello, G.; Barra, D. Evidence for Late Pleistocene uplift at the Somma-Vesuvius apron near Pompeii. *J. Volcanol. Geotherm. Res.* **2011**, *202*, 211–227. [CrossRef]
43. Nicosia, C.; Bonetto, J.; Furlan, G.; Musazzi, S. The pre-79 CE alluvial environment south of Pompeii's city walls. *Geoarchaeology* **2019**, *34*, 727–744. [CrossRef]
44. Amato, V.; Aiello, G.; Barra, D.; Infante, A.; Di Vito, M.A. Nuovi dati geologici per la ricostruzione degli ambienti marino-costieri del 79 d.C. a Pompeii. *Riv. Studi Pompeiani* **2021**, *32*, 103–111.
45. Marturano, A.; Aiello, G.; Barra, D.; Fedele, L.; Grifa, C.; Morra, V.; Berg, R.; Varone, A. Evidence for holocenic uplift at Somma-Vesuvius. *J. Volcanol. Geotherm. Res.* **2009**, *184*, 451–461. [CrossRef]
46. Senatore, M.R.; Ciarallo, A.; Stanley, J.D. Pompeii damaged by volcaniclastic debris flows triggered centuries prior to the 79 AD Vesuvius eruption. *Geoarchaeology* **2014**, *29*, 1–15. [CrossRef]
47. Di Maio, G.; Balassone, G.; Bergamasco, I.; Petrosino, P.; Ricciardi, M.; Stefani, G. Pompeii geoarchaeological setting–An archive older than 40,000 years of volcanism, soil formation and geoarchaeological landscape. *Rend. Online Soc. Geol. Ital.* **2016**, *40*, 865.
48. Ranieri, S. A Contribution to the Study of Stratigrafic Sequence under the AD 79 Layers at Pompeii. *Opusc. Pompeiana* **1998**, *8*, 135–141.
49. Fulford, M.; Wallace-Hadrill, A. Towards a history of pre-Roman Pompeii: Excavations beneath the House of Amarantus (I. 9.11–12), 1995–8. *Pap. Br. Sch. Rome* **1999**, *67*, 37–144. [CrossRef]
50. Robinson, M. La stratigrafia nello studio dell'archeologia preistorica e protostorica a Pompei. In *Nuove Ricerche Sull'area Vesuviana (Scavi 2003–2006), Proceedings of the Atti del Convegno Internazionale, Roma, Italy, 1–3 Febbraio 2007*; Guzzo, P.G., Guidobaldi, M.P., Eds.; Studi della Soprintendenza Archeologica di Pompei; L'Erma di Bretschneider: Roma, Italy, 2008; Volume 25, pp. 125–138.
51. Amato, V. L'approccio geoarcheologico per la ricostruzione crono-stratigrafica del sottosuolo di Pompei: L'esempio dei saggi di scavo all'Insula dei Casti Amanti. In *Ricerche e Scoperte a Pompei: In Ricordo di Enzo Lippolis*; Osanna, M., Ed.; Studi della Soprintendenza Archeologica Pompei; L'Erma di Bretschneider: Roma, Italy, 2021; Volume 45, pp. 117–130.

52. D'Auria, D.; Ballet, P.; Di Vito, M.A.; Russo, A.; Sparice, D. Indagini nel settore meridionale dell'insula I 16 di Pompei. *Fasti Online Doc. Res.* **2023**, *561*, 1–29.
53. Foss, P.W. Rediscovery and resurrection. In *The world of Pompeii*; Dobbins, J.J., Foss, P.W., Eds.; Routledge: New York, NY, USA; London, UK, 2007; pp. 28–42.
54. Spinazzola, V. *Pompeii alla Luce degli Scavi nuovi di Via dell'Abbondanza (Anni 1910–1923)*; Libreria dello Stato: Roma, Italy, 1953; 1110p.
55. Varone, A. *New Finds in Pompeii. The Excavation of Two Buildings in Via dell'Abbondanza*; Apollo: London, UK, 1993; pp. 8–12.
56. Varone, A. Il progetto di scavo e pubblica fruizione dell'insula pompeiana dei Casti Amanti (insula IX 12). In *Nuove Ricerche Archeologiche a Pompei ed Ercolano*; Guzzo, P., Guidobaldi, M.P., Eds.; Electa: Napoli, Italy, 2005; pp. 191–199.
57. de Sanctis, L.; Iovino, M.; Maiorano, R.M.S.; Aversa, S. Seismic stability of the excavation fronts in the ancient Roman city of Pompeii. *Soils Found.* **2020**, *60*, 856–870. [CrossRef]
58. de Sanctis, L.; Maiorano, R.M.S.; Brancaccio, U.; Aversa, S. Geotechnical aspects in the restoration of Insula dei Casti Amanti in Pompeii. *Proc. Inst. Civ. Eng.-Geotech. Eng.* **2019**, *172*, 121–130. [CrossRef]
59. Calvanese, V.; Mighetto, P.; Spinosa, A. Il progetto per l'Insula dei Casti Amanti tra tutela, valorizzazione e fruizione. *E-J. Degli Scavi Pompei* **2024**, *12*, 1–12. Available online: https://pompeiisites.org/wp-content/uploads/12_E-Journal-Insula-dei-Casti-Amanti.pdf (accessed on 28 May 2024).
60. Sbrana, A.; Marianelli, P.; Pasquini, G. Volcanology of Ischia (Italy). *J. Maps* **2018**, *14*, 494–503. [CrossRef]
61. Sbrana, A.; Cioni, R.; Marianelli, P.; Sulpizio, R.; Andronico, D.; Pasquini, G. Volcanic evolution of the Somma-Vesuvius complex (Italy). *J. Maps* **2020**, *16*, 137–147. [CrossRef]
62. Sbrana, A.; Marianelli, P.; Pasquini, G. The phlegrean fields volcanological evolution. *J. Maps* **2021**, *17*, 557–570. [CrossRef]
63. Cioni, R.; Santacroce, R.; Sbrana, A. Pyroclastic deposits as a guide for reconstructing the multi-stage evolution of the Somma-Vesuvius Caldera. *Bull. Volcanol.* **1999**, *61*, 207–222. [CrossRef]
64. Santacroce, R.; Cioni, R.; Marianelli, P.; Sbrana, A.; Sulpizio, R.; Zanchetta, G.; Donahue, D.J.; Joron, J.L. Age and whole rock–glass compositions of proximal pyroclastics from the major explosive eruptions of Somma-Vesuvius: A review as a tool for distal tephrostratigraphy. *J. Volcanol. Geotherm. Res.* **2008**, *177*, 1–18. [CrossRef]
65. Matthews, I.P.; Trincardi, F.; Lowe, J.J.; Bourne, A.J.; MacLeod, A.; Abbott, P.M.; Andersen, N.; Asioli, A.; Blockley, S.P.E.; Lane, C.S.; et al. Developing a robust tephrochronological framework for Late Quaternary marine records in the Southern Adriatic Sea: New data from core station SA03-11. *Quat. Sci. Rev.* **2015**, *118*, 84–104. [CrossRef]
66. Alessandri, L. The early and Middle Bronze Age (1/2) in South and central Tyrrhenian Italy and their connections with the Avellino eruption: An overview. *Quat. Int.* **2019**, *499*, 161–185. [CrossRef]
67. Sevink, J.; Bakels, C.C.; Van Hall, R.L.; Dee, M.W. Radiocarbon dating distal tephra from the Early Bronze Age Avellino eruption (EU-5) in the coastal basins of southern Lazio (Italy): Uncertainties, results, and implications for dating distal tephra. *Quat. Geochronol.* **2021**, *63*, 101154. [CrossRef]
68. Ranieri, S.; Yokoyama, T. The Somma-Vesuvio Eruptions Occurred Between 3760 y. B.P. and AD 79. *Opusc. Pompeiana* **1997**, *7*, 33–50.
69. Andronico, D.; Cioni, R. Contrasting styles of Mount Vesuvius activity in the period between the Avellino and Pompeii Plinian eruptions, and some implications for assessment of future hazards. *Bull. Volcanol.* **2002**, *64*, 372–391. [CrossRef]
70. Rolandi, G.; Petrosino, P.; Mc Geehin, J. The interplinian activity at Somma–Vesuvius in the last 3500 years. *J. Volcanol. Geotherm. Res.* **1998**, *82*, 19–52. [CrossRef]
71. Arnò, V.; Principe, C.; Rosi, M.; Santacroce, R.; Sbrana, A.; Sheridan, M.F. Eruptive history. In *Somma-Vesuvius. Quaderni de 'La Ricerca Scientifica'*; Santacroce, R., Ed.; CNR: Roma, Italy, 1987; Volume 114, pp. 53–103.
72. Orsi, G.; De Vita, S.; Di Vito, M. The restless, resurgent Campi Flegrei nested caldera (Italy): Constraints on its evolution and configuration. *J. Volcanol. Geotherm. Res.* **1996**, *74*, 179–214. [CrossRef]
73. Orsi, G. Volcanic and Deformation History of the Campi Flegrei Volcanic Field, Italy. In *Campi Flegrei. Active Volcanoes of the World*; Orsi, G., D'Antonio, M., Civetta, L., Eds.; Springer: Berlin/Heidelberg, Germany, 2022; pp. 1–53. [CrossRef]
74. De Vivo, B.; Rolandi, G.; Gans, P.B.; Calvert, A.; Bohrson, W.A.; Spera, F.J.; Belkin, H.E. New constrains of pyroclastic eruptive history of the Campanian Volcanic Plain. *Mineral. Petrol.* **2001**, *73*, 47–65. [CrossRef]
75. Giaccio, B.; Hajdas, I.; Isaia, R.; Deino, A.; Nomade, S. High-precision 14C and 40Ar/39Ar dating of the Campanian Ignimbrite (Y-5) reconciles the time-scales of climatic-cultural processes at 40 ka. *Sci. Rep.* **2017**, *7*, 45940. [CrossRef]
76. Deino, A.L.; Orsi, G.; de Vita, S.; Piochi, M. The age of the Neapolitan Yellow Tuff caldera-forming eruption (Campi Flegrei caldera–Italy) assessed by 40Ar/39Ar dating method. *J. Volcanol. Geotherm. Res.* **2004**, *133*, 157–170. [CrossRef]
77. Sparice, D.; Pelullo, C.; de Vita, S.; Arienzo, A.; Petrosino, P.; Mormone, A.; Di Vincenzo, G.; Marfè, B.; Cariddi, B.; De Lucia, M.; et al. The pre-Campi Flegreicaldera (>40 ka) explosive volcanic record in the Neapolitan Volcanic Area: New insights from a scientific drilling north of Naples, southern Italy. *J. Volcanol. Geotherm. Res.* **2024**, *455*, 108209. [CrossRef]
78. Di Vito, M.A.; Isaia, R.; Orsi, G.; Southon, J.D.; De Vita, S.; D'Antonio, M.; Pappalardo, L.; Piochi, M. Volcanism and deformation since 12,000 years at the Campi Flegrei caldera (Italy). *J. Volcanol. Geotherm. Res.* **1999**, *91*, 221–246. [CrossRef]

79. Smith, V.C.; Isaia, R.; Pearce, N.J.G. Tephrostratigraphy and glass compositions of post-15 kyr 76. Campi Flegrei eruptions: Implications for eruption history and chronostratigraphic markers. *Quat. Sci. Rev.* **2011**, *30*, 3638–3660. [CrossRef]
80. Di Vito, M.; Lirer, L.; Mastrolorenzo, G.; Rolandi, G. The 1538 Monte Nuovo eruption (Campi Flegrei, Italy). *Bull. Volcanol.* **1987**, *49*, 608–615. [CrossRef]
81. D'Oriano, C.; Poggianti, E.; Bertagnini, A.; Cioni, R.; Landi, P.; Polacci, M.; Rosi, M. Changes in eruptive style during the AD 1538 Monte Nuovo eruption (Phlegrean Fields, Italy): The role of syn-eruptive crystallization. *Bull. Volcanol.* **2005**, *67*, 601–621. [CrossRef]
82. Vezzoli, L. *Island of Ischia*; Consiglio Nazionale delle Ricerche Quaderni de "La Ricerca Scientifica": Rome, Italy, 1988; Volume 114, p. 122.
83. Brown, R.J.; Orsi, G.; de Vita, S. New insights into Late Pleistocene explosive volcanic activity and caldera formation on Ischia (southern Italy). *Bull. Volcanol.* **2008**, *70*, 583–603. [CrossRef]
84. de Vita, S.; Sansivero, F.; Orsi, G.; Marotta, E.; Piochi, M. Volcanological and structural evolution of the Ischia resurgent caldera (Italy) over the past 10 ky. *Geol. Soc. Am. Spec. Pap.* **2010**, *464*, 193–239. [CrossRef]
85. Cinque, A.; Irollo, G. Il "Vulcano di Pompei": Nuovi dati geomorfologici e stratigrafici. *Alp. Mediterr. Quat.* **2004**, *17*, 101–116.
86. Cinque, A. La trasgressione versiliana nella Piana del Sarno (Campania). *Geogr. Fis. Dinam. Quat.* **1991**, *14*, 63–71.
87. Di Girolamo, P. Un esempio di lava schiuma (foam lava) in Campania (lava schiuma di Pompei scavi). *Rend. Acc. Sci. Fis. Mat.* **1969**, *XXXV*, 3–12.
88. Di Girolamo, P. Lave orvietitiche da trivellazioni nella zona del Somma–Vesuvio. *Rend. Soc. Ital. Mineral. Petrol.* **1969**, *XXV*, 317–345.
89. Kastenmeier, P.; Di Maio, G.; Balassone, G.; Boni, M.; Joachimski, M.; Mondillo, N. The source of stone building materials from the Pompeii archaeological area and its surroundings. *Period. Mineral.* **2010**, *79*, 39–68. [CrossRef]
90. Miriello, D.; Barca, D.; Bloise, A.; Ciarallo, A.; Crisci, G.M.; De Rose, T.; Gattuso, C.; Gazineo, F.; La Russa, M.F. Characterisation of archaeological mortars from Pompeii (Campania, Italy) and identification of construction phases by compositional data analysis. *J. Archaeol. Sci.* **2010**, *37*, 2207–2223. [CrossRef]
91. Dilaria, S.; Previato, C.; Secco, M.; Busana, M.S.; Bonetto, J.; Cappellato, J.; Ricci, G.; Artioli, G.; Tan, P. Phasing the history of ancient buildings through PCA on mortars' mineralogical profiles: The example of the Sarno Baths (Pompeii). *Archaeometry* **2022**, *64*, 866–882. [CrossRef]
92. Franceschini, M.M.N.; Casa, G.; Calandra, S.; Ismaelli, T.; Grifa, C.; Mercurio, M.; Amoretti, V.; Zuchtriegel, G.; Cantisani, E. Raw materials and building technologies in the public buildings of Pompeii after the earthquake of 62/63 CE: A diachronic analysis of mortars. *Case Stud. Constr. Mater.* **2024**, *21*, e03943. [CrossRef]
93. Rolandi, G.; Bellucci, F.; Petrosino, P. The volcanic roots of Pompeii and Herculaneum. In *Volcanism and Archaeology in Mediterranen Area*; Cortini, M., De Vivo, B., Eds.; Research Signpost: Thiruvananthapuram, India, 1997; pp. 89–100.
94. Di Vito, M.A.; Sulpizio, R.; Zanchetta, G.; Calderoni, G. The geology of the South Western slope of Somma-Vesuvius, Italy, as inferred by borehole stratigraphies and cores. *Acta Vulcanol.* **1998**, *10*, 383–393.
95. Di Renzo, V.; Di Vito, M.A.; Arienzo, I.; Carandente, A.; Civetta, L.; D'antonio, M.; Giordano, F.; Orsi, G.; Tonarini, S. Magmatic history of Somma–Vesuvius on the basis of new geochemical and isotopic data from a deep borehole (Camaldoli della Torre). *J. Petrol.* **2007**, *48*, 753–784. [CrossRef]
96. Fisher, R.V.; Orsi, G.; Ort, M.; Heiken, G. Mobility of a large-volume pyroclastic flow—Emplacement of the Campanian ignimbrite, Italy. *J. Volcanol. Geotherm. Res.* **1993**, *56*, 205–220. [CrossRef]
97. Scarpati, C.; Sparice, D.; Perrotta, A. A crystal concentration method for calculating ignimbrite volume from distal ash-fall deposits and a reappraisal of the magnitude of the Campanian Ignimbrite. *J. Volcanol. Geothem. Res.* **2014**, *280*, 67–75. [CrossRef]
98. Scarpati, C.; Sparice, D.; Perrotta, A. Dynamics of large pyroclastic currents inferred by the internal architecture of the Campanian Ignimbrite. *Sci. Rep.* **2020**, *10*, 22230. [CrossRef]
99. Silleni, A.; Giordano, G.; Isaia, R.; Ort, M.H. The magnitude of the 39.8 ka Campanian Ignimbrite eruption, Italy: Method, uncertainties and errors. *Front. Earth Sci.* **2020**, *8*, 543399. [CrossRef]
100. Silleni, A.; Giordano, G.; Ort, M.H.; Isaia, R. Transport and deposition of the 39.8 ka Campanian Ignimbrite large-scale pyroclastic density currents (Italy). *Geol. Soc. Am. Bull.* **2024**, *136*, 4877–4895. [CrossRef]
101. Rittmann, A. Die geologisch bedingte Evolution und Differentiation des Somma–Vesuvius Magmas. *Z. Vulkanol.* **1933**, *15*, 8–94.
102. Giaccio, B.; Isaia, R.; Fedele, F.G.; Di Canzio, E.; Hoffecker, J.; Ronchitelli, A.; Sinitsyn, A.A.; Anikovich, M.; Lisitsyn, S.N.; Popov, V.V. The Campanian Ignimbrite and Codola tephra layers: Two temporal/stratigraphic markers for the Early Upper Palaeolithic in southern Italy and eastern Europe. *J. Volcanol. Geotherm. Res.* **2008**, *177*, 208–226. [CrossRef]
103. Di Vito, M.A.; Sulpizio, R.; Zanchetta, G.; D'Orazio, M. The late Pleistocene pyroclastic deposits of the Campanian Plain: New insights into the explosive activity of Neapolitan volcanoes. *J. Volcanol. Geotherm. Res.* **2008**, *177*, 19–48. [CrossRef]
104. Patti, O. Nuovi dati per la ricerca geo-archeologica dall'Insula dei Casti Amanti (IX, 12). *Riv. Studi Pompeiani* **2003**, *14*, 320–328.
105. Berg, R. Saggi archeologici nell'insula dei Casti Amanti. In Proceedings of the Atti del Convegno Internazionale a Roma, Roma, Italy, 28–30 November 2002; Guzzo, P.G., Guidobaldi, M.P., Eds.; Electa: Napoli, Italy, 2005; pp. 200–215.

106. Berg, R. Saggi stratigrafici nei vicoli a est e a ovest dell'Insula dei Casti Amanti (IX 12). Materia e fasi. In *Nuove Ricerche Archeologiche Nell'area Vesuviana, Scavi 2003–2006*, Proceedings of the Atti del Convegno Internazionale, Roma, Italy, 1–3 February 2007; Guzzo, P.G., Guidobaldi, M.P., Eds.; "L'Erma" di Bretschneider: Rome, Italy, 2008; pp. 363–375.
107. Folk, R.L.; Ward, W.C. Brazos River bar [Texas]; a study in the significance of grain size parameters. *J. Sedim. Res.* **1957**, *27*, 3–26. [CrossRef]
108. Le Bas, M.; Maitre, R.L.; Streckeisen, A.; Zanettin, B.; IUGS Subcommission on the Systematics of Igneous Rocks. A chemical classification of volcanic rocks based on the total alkali-silica diagram. *J. Petrol.* **1986**, *27*, 745–750. [CrossRef]
109. Carracedo Sánchez, M.; Sarrionandia, F.; Arostegui, J.; Eguiluz, L.; Gil Ibarguchi, J.I. The transition of spatter to lava-like body in lava fountain deposits: Features and examples from the Cabezo Segura volcano (Calatrava, Spain). *J. Volcanol. Geotherm. Res.* **2012**, *227–228*, 1–14. [CrossRef]
110. Sparice, D.; Scarpati, C.; Perrotta, A.; Mazzeo, F.C.; Calvert, A.T.; Lanphere, M.A. New insights on lithofacies architecture, sedimentological characteristics and volcanological evolution of pre-caldera (>22 ka), multi-phase, scoria-and spatter-cones at Somma-Vesuvius. *J. Volcanol. Geotherm. Res.* **2017**, *347*, 165–184. [CrossRef]
111. Landi, P.; Bertagnini, A.; Rosi, M. Chemical zoning and crystallization mechanisms in the magma chamber of the Pomici di Base plinian eruption of Somma-Vesuvius (Italy). *Contrib. Mineral. Petrol.* **1999**, *135*, 179–197. [CrossRef]
112. Melluso, L.; Scarpati, C.; Zanetti, A.; Sparice, D.; de' Gennaro, R. The petrogenesis of chemically zoned, phonolitic, Plinian and sub-Plinian eruptions of Somma-Vesuvius, Italy: Role of accessory phase removal, independently filled magma reservoirs with time, and transition from slightly to highly silica undersaturated magmatic series in an ultrapotassic stratovolcano. *Lithos* **2022**, *430–431*, 106854. [CrossRef]
113. Bertagnini, A.; Landi, P.; Rosi, M.; Vigliargio, A. The Pomici di Base plinian eruption of Somma-Vesuvius. *J. Volcanol. Geotherm. Res.* **1998**, *83*, 219–239. [CrossRef]
114. Orsi, G.; Civetta, L.; D'Antonio, M.; Di Girolamo, P.; Piochi, M. Step-filling and development of a three-layer magma chamber: The Neapolitan Yellow Tuff case history. *J. Volcanol. Geotherm. Res.* **1995**, *67*, 291–312. [CrossRef]
115. Wohletz, K.; Orsi, G.; De Vita, S. Eruptive mechanisms of the Neapolitan Yellow Tuff interpreted from stratigraphic, chemical, and granulometric data. *J. Volcanol. Geotherm. Res.* **1995**, *67*, 263–290. [CrossRef]
116. Forni, F.; Petricca, E.; Bachmann, O.; Mollo, S.; De Astis, G.; Piochi, M. The role of magma mixing/mingling and cumulate melting in the Neapolitan Yellow Tuff caldera-forming eruption (Campi Flegrei, Southern Italy). *Contrib. Mineral. Petrol.* **2018**, *173*, 1–18. [CrossRef]
117. Aulinas, M.; Civetta, L.; Di Vito, M.A.; Orsi, G.; Gimeno, D.; Férnandez-Turiel, J.L. The "Pomici di mercato" Plinian eruption of Somma-Vesuvius: Magma chamber processes and eruption dynamics. *Bull. Volcanol.* **2008**, *70*, 825–840. [CrossRef]
118. D'Antonio, M.; Civetta, L.; Orsi, G.; Pappalardo, L.; Piochi, M.; Carandente, A.; de Vita, S.; Di Vito, M.A.; Isaia, R. The present state of the magmatic system of the Campi Flegrei caldera based on a reconstruction of its behavior in the past 12 ka. *J. Volcanol. Geotherm. Res.* **1999**, *91*, 247–268. [CrossRef]
119. Lustrino, M.; Marturano, A.; Morra, V.; Ricci, G. Volcanological and geochemical features of young pyroclastic levels (<12 ka) in the urban area of Naples (S. Italy). *Per. Mineral.* **2002**, *71*, 241–253.
120. Forni, F.; Degruyter, W.; Bachmann, O.; De Astis, G.; Mollo, S. Long-term magmatic evolution reveals the beginning of a new caldera cycle at Campi Flegrei. *Sci. Adv.* **2018**, *4*, eaat9401. [CrossRef] [PubMed]
121. Sulpizio, R.; Cioni, R.; Di Vito, M.A.; Mele, D.; Bonasia, R.; Dellino, P. The Pomici di Avellino eruption of Somma-Vesuvius (3.9 ka BP). Part I: Stratigraphy, compositional variability and eruptive dynamics. *Bull. Volcanol.* **2010**, *72*, 539–558. [CrossRef]
122. Balcone-Boissard, H.; Boudon, G.; Ucciani, G.; Villemant, B.; Cioni, R.; Civetta, L.; Orsi, G. Magma degassing and eruption dynamics of the Avellino pumice Plinian eruption of Somma–Vesuvius (Italy). Comparison with the Pompeii eruption. *Earth Planet. Sci. Lett.* **2012**, *331*, 257–268. [CrossRef]
123. Cioni, R.; Sulpizio, R.; Garruccio, N. Variability of the eruption dynamics during a subplinian event: The Greenish Pumice eruption of Somma–Vesuvius (Italy). *J. Volcanol. Geotherm. Res.* **2003**, *124*, 89–114. [CrossRef]
124. Scarpati, C.; Cole, P.; Perrotta, A. The Neapolitan Yellow Tuff—A large volume multiphase eruption from Campi Flegrei, southern Italy. *Bull. Volcanol.* **1993**, *55*, 343–356. [CrossRef]
125. Crocitti, M.; Sulpizio, R.; Insinga, D.D.; De Rosa, R.; Donato, P.; Iorio, M.; Zanchetta, G.; Barca, D.; Lubritto, C. On ash dispersal from moderately explosive volcanic eruptions: Examples from Holocene and Late Pleistocene eruptions of Italian volcanoes. *J. Volcanol. Geotherm. Res.* **2019**, *385*, 198–221. [CrossRef]
126. Totaro, F.; Insinga, D.D.; Lirer, F.; Margaritelli, G.; Caparrós, A.C.; de la Fuente, M.; Petrosino, P. The Late Pleistocene to Holocene tephra record of ND14Q site (southern Adriatic Sea): Traceability and preservation of Neapolitan explosive products in the marine realm. *J. Volcanol. Geotherm. Res.* **2022**, *423*, 107461. [CrossRef]
127. Mele, D.; Sulpizio, R.; Dellino, P.; La Volpe, L. Stratigraphy and eruptive dynamics of a pulsating Plinian eruption of Somma-Vesuvius: The Pomici di Mercato (8900 years BP). *Bull. Volcanol.* **2011**, *73*, 257–278. [CrossRef]
128. Taddeucci, J.; Alatorre-Ibargüengoitia, M.A.; Cruz-Vázquez, O.; Del Bello, E.; Scarlato, P.; Ricci, T. In-flight dynamics of volcanic ballistic projectiles. *Rev. Geophys.* **2017**, *55*, 675–718. [CrossRef]

129. Bisson, M.; Spinetti, C.; Gianardi, R.; Strehlow, K.; De Beni, E.; Landi, P. High-resolution mapping and dispersion analyses of volcanic ballistics emitted during the 3rd July 2019 paroxysm at Stromboli. *Sci. Rep.* **2023**, *13*, 13465. [CrossRef] [PubMed]
130. Houghton, B.F.; Wilson, C.J.N.; Fierstein, J.; Hildreth, W. Complex proximal deposition during the Plinian eruptions of 1912 at Novarupta, Alaska. *Bull. Volcanol.* **2004**, *66*, 95–133. [CrossRef]
131. Houghton, B.; Carey, R.J. Pyroclastic Fall Deposits. In *The Encyclopedia of Volcanoes*; Sigurdsson, H., Ed.; Academic Press: Cambridge, MA, USA, 2015; pp. 599–616. [CrossRef]
132. Scarpati, C.; Sparice, D.; Perrotta, A. Comparative proximal features of the main Plinian deposits (Campanian Ignimbrite and Pomici di Base) of Campi Flegrei and Vesuvius. *J. Volcanol. Geotherm. Res.* **2016**, *321*, 149–157. [CrossRef]
133. Passariello, I.; Lubritto, C.; D'Onofrio, A.; Guan, Y.; Terrasi, F. The Somma–Vesuvius complex and the Phlaegrean Fields caldera: New chronological data of several eruptions of the Copper–Middle Bronze Age period. *Nucl. Instrum. Methods Phys. Res. Sect. B* **2010**, *268*, 1008–1012. [CrossRef]
134. Peccerillo, A. *Plio-Quaternary Volcanism in Italy*; Springer: Berlin/Heidelberg, Germany, 2005; pp. 1–365.
135. D'Oriano, C.; Bertagnini, A.; Cioni, R. Eruptive scenario of ash-dominated events at Vesuvius: The AP3 eruption (2,710±60 years BP). *Acta Vulcanol. J. Natl. Volcan. Group Italy* **2010**, *22*, 107–122.
136. Fedele, F.G.; Giaccio, B.; Isaia, R.; Orsi, G. The Campanian Ignimbrite eruption, Heinrich Event 4, and Paleolithic change in Europe: A high-resolution investigation. *Geophys. Monogr. Am. Geophys. Union* **2003**, *139*, 301–328. [CrossRef]
137. Fedele, F.G.; Giaccio, B.; Hajdas, I. Timescales and cultural process at 40,000 BP in the light of the Campanian Ignimbrite eruption, Western Eurasia. *J. Hum. Evol.* **2008**, *55*, 834–857. [CrossRef] [PubMed]
138. Head, J.W.; Wilson, L. Basaltic pyroclastic eruptions: Influence of gas-release patterns and volume fluxes on fountain structure, and the formation of cinder cones, spatter cones, rootless flows, lava ponds and lava flows. *J. Volcanol. Geotherm. Res.* **1989**, *37*, 261–271. [CrossRef]
139. Sumner, J.M.; Blake, S.; Matela, R.J.; Wolff, J.A. Spatter. *J. Volcanol. Geotherm. Res.* **2005**, *142*, 49–65. [CrossRef]
140. Taddeucci, J.; Edmonds, M.; Houghton, B.; James, M.R.; Vergniolle, S. Hawaiian and Strombolian eruptions. In *The Encyclopedia of Volcanoes*; Sigurdsson, H., Ed.; Academic Press: Cambridge, MA, USA, 2015; pp. 485–503.
141. Mellors, R.A.; Sparks, R.S.J. Spatter-rich pyroclastic flow deposits on Santorini, Greece. *Bull. Volcanol.* **1991**, *53*, 327–342. [CrossRef]
142. Branney, M.J.; Kokelaar, B.P.; McConnell, B.J. The Bad Step Tuff: A lava-like rheomorphic ignimbrite in a calc-alkaline piecemeal caldera, English Lake District. *Bull. Volcanol.* **1992**, *54*, 187–199. [CrossRef]
143. Perrotta, A.; Scarpati, C. The dynamics of the Breccia Museo eruption (Campi Flegrei, Italy) and the significance of spatter clasts associated with lithic breccias. *J. Volcanol. Geotherm. Res.* **1994**, *59*, 335–355. [CrossRef]
144. Valentine, G.A.; Perry, F.V.; WoldeGabriel, G. Field characteristics of deposits from spatter-rich pyroclastic density currents at Summer Coon volcano, Colorado. *J. Volcanol. Geotherm. Res.* **2000**, *104*, 187–199. [CrossRef]
145. Allen, S.R. Complex spatter-and pumice-rich pyroclastic deposits from an andesitic caldera-forming eruption: The Siwi pyroclastic sequence, Tanna, Vanuatu. *Bull. Volcanol.* **2004**, *67*, 27–41. [CrossRef]
146. Kokelaar, P.; Raine, P.; Branney, M.J. Incursion of a large-volume, spatter-bearing pyroclastic density current into a caldera lake: Pavey Ark ignimbrite, Scafell caldera, England. *Bull. Volcanol.* **2007**, *70*, 23–54. [CrossRef]
147. Martin, A.P.; Smellie, J.L.; Cooper, A.F.; Townsend, D.B. Formation of a spatter-rich pyroclastic density current deposit in a Neogene sequence of trachytic-mafic igneous rocks at Mason Spur, Erebus volcanic province, Antarctica. *Bull. Volcanol.* **2018**, *80*, 13. [CrossRef]
148. Capaccioni, B.; Cuccoli, F. Spatter and welded air fall deposits generated by fire-fountaining eruptions: Cooling of pyroclasts during transport and deposition. *J. Volcanol. Geotherm. Res.* **2005**, *145*, 263–280. [CrossRef]
149. Rader, E.; Geist, D. Eruption condition of spatter deposits. *J. Volcanol. Geotherm. Res.* **2015**, *304*, 287–293. [CrossRef]
150. Rader, E.; Kobs Nawotniak, S.; Heldmann, J. Variability of spatter morphology in pyroclastic deposits in southern Idaho, as correlated to thermal conditions and eruptive environment. *Earth Space Sci.* **2018**, *5*, 592–603. [CrossRef]
151. Rader, E.; Wysocki, R.S.; Heldmann, J.; Harpp, K.; Bosselait, M.; Myers, M. Spatter stability: Constraining accumulation rates and temperature conditions with experimental bomb morphology. *Bull. Volcanol.* **2020**, *82*, 49. [CrossRef]
152. Macdonald, R.; Bagiński, B.; Rolandi, G.; De Vivo, B.; Kopczyńska, A. Petrology of parasitic and eccentric cones on the flanks and base of Somma-Vesuvius. *Mineral. Petrol.* **2016**, *110*, 65–85. [CrossRef]
153. Amato, V.; Aucelli, P.P.C.; D'Argenio, B.; Da Prato, S.; Ferraro, L.; Pappone, G.; Petrosino, P.; Rosskopf, C.M.; Ermolli, E.R. Holocene environmental evolution of the costal sector in front of the Poseidonia-Paestum archaeological area (Sele plain, southern Italy). *Rend. Lincei* **2012**, *23*, 45–59. [CrossRef]
154. Munno, R.; Petrosino, P. Tephra layers in the S. Gregorio Magno lacustrine succession. *J. Quat. Sci.* **2007**, *22*, 247–266. [CrossRef]
155. Ippolito, F. Segnalazione di un pozzo esistente nell'antica città di Pompei. *Boll. Soc. Nat. Napoli* **1938**, *49*, 3–8.
156. Orschiedt, J. The Late Upper Palaeolithic and earliest Mesolithic evidence of burials in Europe. *Philos. Trans. R. Soc. Lond. Ser. B* **2018**, *373*, 20170264. [CrossRef] [PubMed]
157. Ellis, S.J.; Emmerson, A.L.; Pavlick, A.K.; Dicus, K. The 2010 field season at I. 1.1-10, Pompeii: Preliminary report on the excavations. *FOLD&R* **2011**, *220*, 1–17.

158. Robinson, M.; Trümper, M.; Brünenberg, C.; Dickmann, J.A.; Esposito, D.; Ferrandes, A.F.; Pardini, G.; Pegurri, A.; Rummel, C. Stabian Baths in Pompeii. New Research on the Archaic Defenses of the City. *Archäologischer Anz.* **2021**, *2*, 1–65. [CrossRef]
159. Osanna, M.; Alessi, D.; De Candia, R. La Scuola Superiore Meridionale a Pompei. Indagini lungo il Portico Orientale del Foro Triangolare: Campagna di scavo 2022. *Quad. ACMA* **2024**, *2*, 155–172. [CrossRef]
160. Vingiani, S.; Minieri, L.; Albore Livadie, C.; Di Vito, M.A.; Terribile, F. Pedological investigation of an early Bronze Age site in southern Italy. *Geoarchaeology* **2017**, *33*, 193–217. [CrossRef]
161. Pluciennik, M. Radiocarbon Determinations and the Mesolithic-Neolithic transition in southern Italy. *J. Med. Archaeol.* **1997**, *10*, 115–150. [CrossRef]
162. Natali, E.; Forgia, V. The beginning of the Neolithic in Southern Italy and Sicily. *Quat. Int.* **2018**, *470*, 253–269. [CrossRef]
163. Passariello, I.; Livadie, C.A.; Talamo, P.; Lubritto, C.; D'Onofrio, A.; Terrasi, F. ^{14}C chronology of Avellino pumices eruption and timing of human reoccupation of the devastated region. *Radiocarbon* **2009**, *51*, 803–816. [CrossRef]
164. Di Vito, M.A.; Castaldo, N.; De Vita, S.; Bishop, J.; Vecchio, G. Human colonization and volcanic activity in the eastern Campania Plain (Italy) between the Eneolithic and Late Roman periods. *Quat. Int.* **2013**, *303*, 132–141. [CrossRef]
165. Pappalardo, U. Vesuvio: Grandi eruzioni e reinsediamenti. In *Modalità Insediative e Strutture Agrarie Nell'italia Meridionale in Età Romana*; Lo Cascio, E., Storchi Marino, A., Eds.; Edipuglia: Bari, Italy, 2002; pp. 435–453.
166. Sulpizio, R.; Bonasia, R.; Dellino, P.; Mele, D.; Di Vito, M.A.; La Volpe, L. The Pomici di Avellino eruption of Somma–Vesuvius (3.9 ka BP). Part II: Sedimentology and physical volcanology of pyroclastic density current deposits. *Bull. Volcanol.* **2010**, *72*, 559–577. [CrossRef]
167. Russo, F. I siti archeologici del Bronzo Antico in Campania interessati dall'eruzione vesuviana delle" Pomici di Avellino": Elementi geomorfologici e stratigrafici. *Territ. Stor. Ambiente* **1999**, *2*, 93–118.
168. Russo, F.; Valente, A. L'impatto delle eruzioni tardo oloceniche del Somma-Vesuvio sul paesaggio e le attività umane. Una sintesi di dati geoarcheologici. *Boll. Soc. Geogr. Italy* **2010**, *3*, 583–604.
169. Matarazzo, T.; Berna, F.; Goldberg, P. Occupation surfaces sealed by the Avellino eruption of Vesuvius at the Early Bronze Age village of Afragola in southern Italy: A micromorphological analysis. *Geoarchaeology* **2010**, *25*, 437–466. [CrossRef]
170. Di Lorenzo, H.; Di Vito, M.A.; Talamo, P.; Bishop, J.; Castaldo, N.; de Vita, S.; Nave, R.; Pacciarelli, M. The impact of the Pomici di Avellino Plinian eruption of Vesuvius on Early and Middle Bronze Age human settlement in Campania (southern Italy). *Tagungen Landesmus. Vorgesch. Halle* **2013**, *9*, e265.
171. Albore Livadie, C.; Campajola, L.; D'Onofrio, A.; Moniot, R.; Roca, V.; Romano, M.; Russo, F.; Terrasi, F. Evidence of the adverse impact of the «Avellino Pumices» eruption of Somma-Vesuvius on old bronze age sites in the Campania region (Southern Italy). *Quaternaire* **1998**, *9*, 37–43. [CrossRef]
172. Albore Livadie, C.; Pearce, M.; Delle Donne, M.; Pizzano, N. The effects of the Avellino Pumice eruption on the population of the Early Bronze age Campanian plain (Southern Italy). *Quat. Int.* **2019**, *499*, 205–220. [CrossRef]
173. Nilsson, M. The first of a series of Disasters? Pompeii and the aftermath of an early bronze age eruption. *Archaeol. Rev. Camb.* **2009**, *24*, 81–98.
174. Mastroroberto, M. La necropoli di Sant'Abbondio: Una comunità dell'età del Bronzo a Pompei. In *Archeologia e Vulcanologia in Campania*; Guzzo, P.G., Peroni, R., Eds.; Arte Tipografica: Pompei, Italy, 1998; pp. 135–149.
175. Mastroroberto, M.; Talamo, P. Il sito di Sant'Abbondio a Pompei: Continuità e trasformazione tra Bronzo Antico e Bronzo Medio. In *Pompei-Scienza e Società, Proceedings of the 250° Anniversario degli Scavi di Pompei–Convegno Internazionale, Napoli, Italy, 25–27 November 1998*; Guzzo, P.G., Ed.; Electa: Milano, Italy, 2001; Volume 2, p. 208.
176. Calderoni, G.; Russo, F. Geoarchaeological stratigraphy and radiocarbon datings of a deposit from a site of the Pompeian area (Campania, Southern Italy). *Alp. Mediterr. Quat.* **2006**, *19*, 261–268.
177. Pappalardo, U.; Russo, F.; Mastroroberto, M.; Calderoni, G. La necropoli dell'Età del Bronzo di Sant'Abbondio a Pompei dati geomorfologico-stratigrafici ed archeologici. *Riv. Studi Pompeiani* **2017**, *28*, 146–152.
178. Albore Livadie, C.; D'Alessio, G.; Mastrolorenzo, G.; Rolandi, G. Le eruzioni del Somma-Vesuvio in epoca protostorica. In *Tremblement de Terre, Éruptions Volcaniques et Vié des Hommes dans la Campanie Antique*; Centre J Bérard–Bibliothèque de l'Institute Francais de Naples Deuxième Série: Naples, Italy, 1986; Volume VII, pp. 55–66. [CrossRef]
179. Cioni, R.; Bertagnini, A.; Santacroce, R.; Andronico, D. Explosive activity and eruption scenarios at Somma-Vesuvius (Italy): Towards a new classification scheme. *J. Volcanol. Geotherm. Res.* **2008**, *178*, 331–346. [CrossRef]

Disclaimer/Publisher's Note: The statements, opinions and data contained in all publications are solely those of the individual author(s) and contributor(s) and not of MDPI and/or the editor(s). MDPI and/or the editor(s) disclaim responsibility for any injury to people or property resulting from any ideas, methods, instructions or products referred to in the content.